A PULSE MODULATED LASER COMMUNICATIONS SYSTEM

John James Sulfaro

NAVAL POSTGRADUATE SCHOOL
Monterey, California

THESIS

A PULSE MODULATED

LASER COMMUNICATIONS SYSTEM

by

John James Sulfaro

December 1974

Thesis Advisor: C. H. Rothauge

REPORT DOCUMENTATION PAGE

READ INSTRUCTIONS BEFORE COMPLETING FORM

1. REPORT NUMBER	2. GOVT ACCESSION NO. / 3. RECIPIENT'S CATALOG NUMBER
4. TITLE (and Subtitle): A Pulse Modulated Laser Communications System	5. TYPE OF REPORT & PERIOD COVERED: Master's Thesis; December 1974
	6. PERFORMING ORG. REPORT NUMBER
7. AUTHOR(s): John James Sulfaro	8. CONTRACT OR GRANT NUMBER(s)
9. PERFORMING ORGANIZATION NAME AND ADDRESS: Naval Postgraduate School, Monterey, California 93940	10. PROGRAM ELEMENT, PROJECT, TASK AREA & WORK UNIT NUMBERS
11. CONTROLLING OFFICE NAME AND ADDRESS: Naval Postgraduate School, Monterey, California 93940	12. REPORT DATE: December 1974
	13. NUMBER OF PAGES: 67
14. MONITORING AGENCY NAME & ADDRESS (if different from Controlling Office): Naval Postgraduate School, Monterey, California 93940	15. SECURITY CLASS. (of this report): Unclassified
	15a. DECLASSIFICATION/DOWNGRADING SCHEDULE

16. DISTRIBUTION STATEMENT (of this Report)

Approved for public release; distribution unlimited.

17. DISTRIBUTION STATEMENT (of the abstract entered in Block 20, if different from Report)

18. SUPPLEMENTARY NOTES

19. KEY WORDS (Continue on reverse side if necessary and identify by block number)

Laser Communications System

20. ABSTRACT (Continue on reverse side if necessary and identify by block number)

A system for line-of-sight voice communications using Laser technology as the information carrier was constructed. Photodiode detection techniques were used in the receiver section. Emphasis was placed on compactness so maximum utilization of Integrated circuits was made. A one-way communications system was built.

A Pulse Modulated

Laser Communications System

by

John James Sulfaro
Lieutenant, United States Navy
B.S., United States Naval Academy, 1966

Submitted in partial fulfillment of the
requirements for the degree of

MASTER OF SCIENCE IN ELECTRICAL ENGINEERING

from the

NAVAL POSTGRADUATE SCHOOL
December 1974

ABSTRACT

A system for line-of-sight voice communications using Laser technology as the information carrier was constructed. Photodiode detection techniques were used in the receiver section. Emphasis was placed on compactness so maximum utilization of Integrated cirucits was made. A one-way communications system was built.

TABLE OF CONTENTS

LIST OF DRAWINGS

I. INTRODUCTION

A. OBJECTIVE

The objective of this research was to design, construct and test a workable pulsed laser communications system. The concept could be employed for secure communications as on the flight decks of aircraft carriers.

B. HISTORY

1. The field of laser communications has developed from the infancy stages of the early 1960's to the present position as one of the more promising communications fields of the future. Presently many different type laser systems are operating utilizing both open and closed mediums of transmission. Several early systems were developed for the Navy utilizing a hand held receiver transmitter for short range ship to ship communication primarily for use in ship to ship refueling evolutions.

The advantages of such a system are many in that it allows communications amongst selected ships with little or no possibility of detection by opposing forces. The ability to concentrate the transmitted energy in a narrow beam reduces the possibility of interception.

The Naval Electronics Laboratory Center used refined laser communications techniques to enable an aircraft to communicate with friendly submarines or to interrogate one of unknown origin [Ref. 1].

2. With a widening selection of components from integrated chips to transceivers, the communications designer can consider a laser system as a smaller, less expensive choice over microwave for such applications as secure communications, intrusion detection and remote control. The laser offers superior data-rate capacity of 100 kHz through several miles of atmosphere. With pulse-position and pulse-interval modulation, the pulsed laser is compatible with existing computers and other data systems for both narrow and wide-band communications.

Because it's energy can be concentrated in nanosecond pulses, a laser signal can be detected with a simple threshold receiver instead of the complex heterodyne receiver required for background suppression and doppler compensation with microwave oscillators. In addition the pulsed system's low duty cycle permits inter-leaving of pulses of the same wavelength, simplifying the selection of transmitter and lock-on amplifiers.

The most promising use of lasers in communications lies in the field of fiber optics. With the advent of low loss commercial optical fibers, coherent and incoherent laser sources are rapidly becoming one of the most efficient means of transmitting data. Utilizing any of the modulating schemes available, lasers are converting electrical signals to optical signals for transmission through optical fiber cables. High data rates and secure transmission of information make the laser/optical fiber team very attractive

when compared to the conventional coaxial cable transmission lines.

The U. S. Navy has expressed great interest in this area with ongoing development programs for multi-station data transmission over fiber optic cables. Inter-ship communications experiments have been conducted as well as extensive environmental tests. Tests have also been completed with fiber optic bundles as the transmission medium in the Navy's message processing and distribution systems (MPDS). Numerous closed circuit television systems utilizing fiber optic cabling have been tested. These systems used light emitting diodes (LED's) as the light source.

The Cable Television Industry (CATV) also expressed great interest in the LED/fiber optic team as the transmission medium in their studies of a wired city concept of communications.

II. THE LASER COMMUNICATIONS SYSTEM

A. THEORY OF OPERATION

The design of the system was limited by the fact that the available laser transmitter had a maximum pulse repetition frequency of 10 kHz. It was desired to transmit acceptable audio signals so the audio signal was limited to a 100-3000 Hz bandwidth. In order to maximize the separation of the carrier frequency from the audio, a 7 kHz carrier was selected. The laser transmitter would be pulsed by a voltage-controlled oscillator (VCO) which is varied by the input voltage of the audio signal. The signal is detected by a photodiode and demodulated in a phase-locked loop (PLL) demodulator, filtered and amplified for an audio output.

B. TRANSMITTER DESCRIPTION

The transmitter converts the audio input signal into a pulse-modulated optical signal output. The microphone converts the audio signal to time-varying voltages which in turn are amplified and filtered in a high gain notch filter. The gain of the filter was limited to keep VCO within the desired output frequencies thus negating the need for an attenuator or automatic gain control (AGC) circuitry. The low frequency response of the microphone is limited to 100 Hz forming the lower limit of our filter network while the notch filter design has a 17 db attenuation at 3000 Hz as shown in Figure 9.

The VCO transfer characteristics are shown in Figure 12. Utilizing basic FM deviation theory, it is easy to demonstrate that the maximum modulation should be ±1450 Hz.

The carrier frequency is increased during half of the modulating signal and decreased during the half cycle of opposite polarity. The change in the carrier frequency (frequency deviation) is proportional to the instantaneous amplitude of the modulating signal, so the deviation is small when the instantaneous amplitude of the modulating signal reaches it's peak either positive or negative.

The ratio between the frequency deviation (in Hz), and the modulating frequency (also in Hz), is called the modulating index. That is,

$$\text{Modulation Index} = \frac{\text{Carrier frequency deviation}}{\text{Modulation frequency}} .$$

In an FM system, the ratio of the maximum carrier frequency deviation to the highest modulating frequency used is called the deviation ratio [Ref. 2].

Utilizing Carsons Rule,

$$B = 2(\Delta f + f_m) \simeq 2\Delta f_{max}$$

$$= 2(1450 + 3000) = 8900\text{Hz}$$

the required bandwidth of the system was clearly determined to be less than the 10 kHz pulse repetition rate constraint.

C. RECEIVER DESCRIPTION

The receiver utilized a photodiode, which supplied a frequency varying signal to the PLL demodulator, to detect

the modulated light signals of the transmitter. The PLL demodulates the frequency varying signal and produces a voltage varying signal at the output. The PLL utilizes a 7 kHz center frequency as did the VCO. A notch filter with 32 db of attenuation at the 7 kHz center frequency was employed to remove the undesired signals caused by the close proximity of the carrier frequency to the audio bandwidth.

D. THE LASER TRANSMITTER

The laser transmitter utilized combined the laser diode, the trigger networks and a collimating lens in one package. The transmitter utilizes a Gallium Arsenide laser diode coupled with a Schmitt trigger pulse forming circuit to provide emission at relatively high repetition rates. The laser is equipped with a collimating lens to provide for the projection of the optical beam over great distances. It was triggerable from an external source so that pulse position frequency modulation can be applied as desired.

A semiconductor laser consists of essentially a very small sample of chip of semiconductor material, often (though not always) in the form of a p-n junction diode. When some of the electrons in a semiconductor sample are excited from the valence band into the conduction band (for example, by shining light on the sample, bombarding it with an electron beam, or passing current through it), it is often possible to observe a band-gap emission, or radiative recombination, from the semiconductor at wavelengths more or less corresponding to the energy gap between

valence and conduction bands. This radiation is floures-cence, or spontaneous emission, caused by some of the excess electrons in the conduction band dropping back down to the valence band and giving up their excess energy as light in the process. If such a semiconductor sample can be pumped strongly enough, by bombarding it strongly or passing very large forward currents through the p-n junction, it becomes possible to obtain a population inversion between certain of the valence and conduction levels and thus to observe a genuine laser action at these wavelengths.

Laser action can now be obtained in this way in a dozen or more semiconductor materials at numerous wavelengths ranging from the visible and ultraviolet to about 10 micron in the infrared region, depending upon the semiconductor band gaps available. Pumping with a high voltage electron beam is the most effective excitation method and leads to laser action in the largest number of materials. However, we will concentrate chiefly on the d-c current excited p-n junction type of semiconductor laser, since it is by far the simplest and most useful type. This form of semi-conductor laser is sometimes called the injection or diode injection laser, since the laser action is created by charge carriers injected into a semiconductor diode.

Figure 1 shows the structure of a typical diode-injec-tion laser, the diode itself is a tiny chip of semiconductor material such as gallium arsenide (Ga As), typically between .3 and 1 mm (12 to 40 mils) long and with even smaller transverse dimensions, soldered onto a small gold-plated

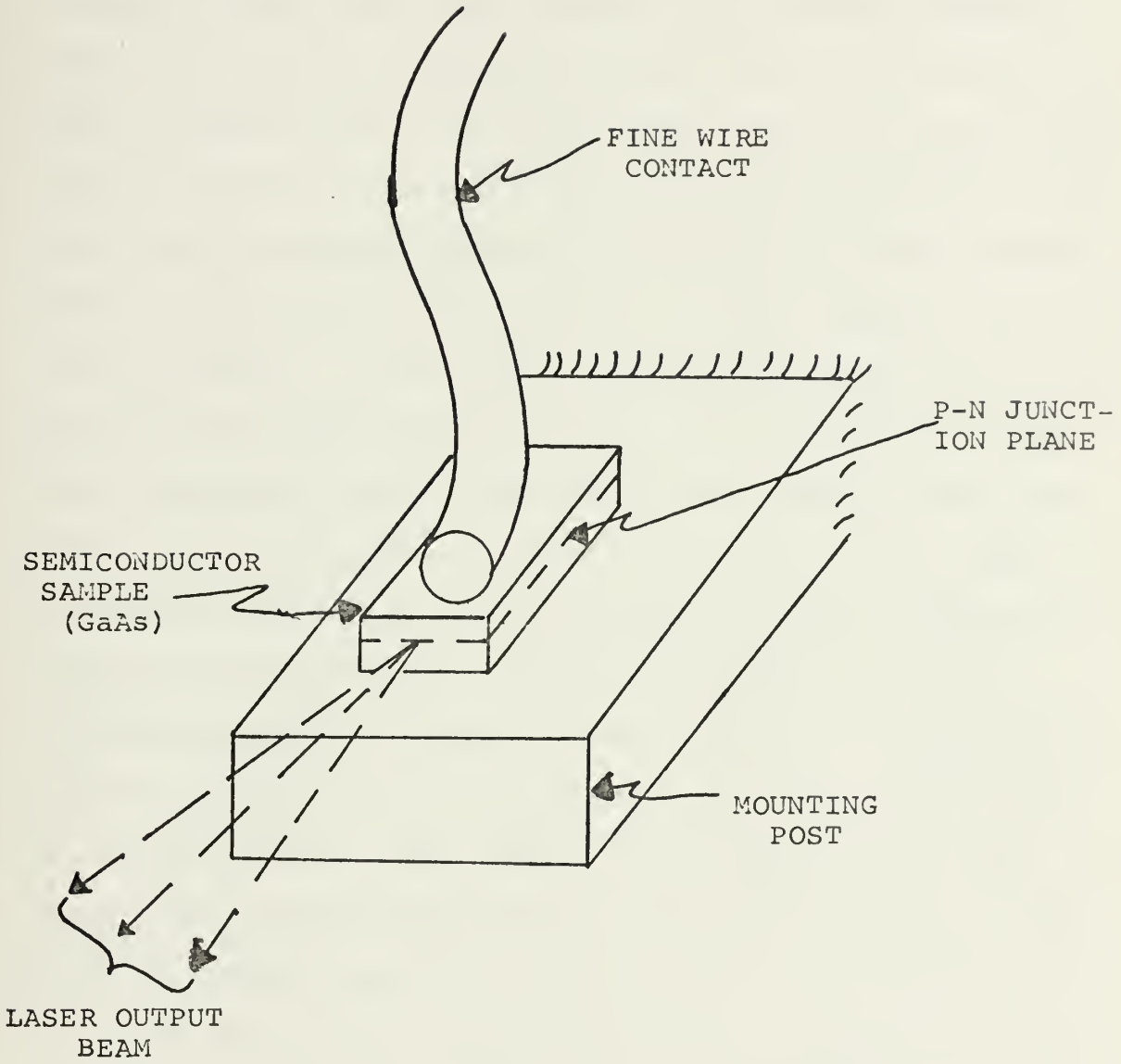

FIGURE 1 A TYPICAL DIODE-INJECTION LASER STRUCTURE

mounting post or tab. The sample is cut from heavily doped n-type material, but only after p-type impurities have been diffused into the top of the sample, so that the top layer becomes p-type with a thin, planar p-n junction created a short distance below the top surface. Contact to the p region is made by means of a fine line. When a large forward current is passed through this diode, population inversion and laser action are created in a very thin layer, perhaps only 10 microns thick, located at or very close to the junction plane. If the ends of the diode sample are cut by cleaving the semiconductor crystal, they provide extremely smooth parallel surfaces without further preparation, and since the laser gain in the junction layer is very high, the normal reflection (~ 30 percent) at the semiconductor air end surface provides sufficient feedback for laser oscillation without further mirror coating. The laser output then emerges from the junction plane through the ends of the small chip. The sides of the sample are usually rough sawn to inhibit undesired reflections from the side surfaces of the crystal.

In discussing the general principles of semiconductor recombination radiation and injection laser action, some familiarity with semiconductor theory and the allowed energy levels for electrons in semiconductors is assumed. These levels are grouped into broad bands, generally with energy gaps between certain bands; in particular, there is normally a valence band, separated by an energy gap from higher-lying conduction bands. Under normal conditions

in an intrinsic or undoped semiconductor, virtually all the available energy levels in the valence band are occupied by electrons, and the conduction band is virtually empty; i.e., very few electrons have sufficient energy from thermal or other sources to occupy levels in the conduction band. If there are any unfilled energy levels near the top of the valence band, the vacancy or deficit of a negatively charged electron in such an energy level acts as a mobile positive-charge carrier and is called a hole. The energy gap between the valence and conduction bands is the characteristic energy gap or band gap of the semiconductor. The band gap generally corresponds by Planck's law, to a frequency or wavelength in the visible or infrared region of the spectrum.

In a nonintrinsic doped semiconductor, there will be a number of additional rather sharply defined energy levels located within the energy gap, due to the presence of various added impurities or doping atoms in the semiconductor. If these added energy levels are located just above the top of the valence band and can accept additional electrons, the impurities are called acceptors and the semiconductor becomes a p-type. If the added levels are located just below the bottom of the conduction band and have electrons to give up, the impurities are called donors and the semiconductor becomes an n-type. In lightly doped semiconductors the acceptor or donor levels form rather sharp and distinct energy levels within the band gap. Injection lasers, however, more commonly use heavily doped materials, in which the acceptor and donor energy levels broaden and more or

less merge with the closely adjacent valence or conduction bands, respectively.

Figure 2 shows energy level diagrams describing the valence band and conduction bands in the p-n junction region of a heavily doped sample. An important parameter is a semiconductor at thermal equilibrium is the Fermi energy level. This energy level is a parameter in the Fermi-Dirac statistical distribution of electrons among the available energy levels, but it also represents physically the energy level below which essentially all available levels are occupied and above which essentially all levels are empty. With no voltage applied, the Fermi level must be constant everywhere throughout a semiconductor sample. Figure 2 shows the resulting energy level diagram near a p-n junction between heavily doped n and p regions at equilibrium with no voltage applied. On the n side, both the conduction band and the occupied donor energy levels are filled, and hence on an absolute energy scale the entire energy-level structure must be depressed slightly below the Fermi level E_f, as shown. Conversely, on the p side the acceptor-created energy levels of the top of the valence band are not filled, and the entire band structure must be located slightly above the Fermi level. The intervening region between the p and n regions is the transition or junction region. The absolute energy difference between the p and n regions is the built-in voltage or contact potential of the p-n diode.

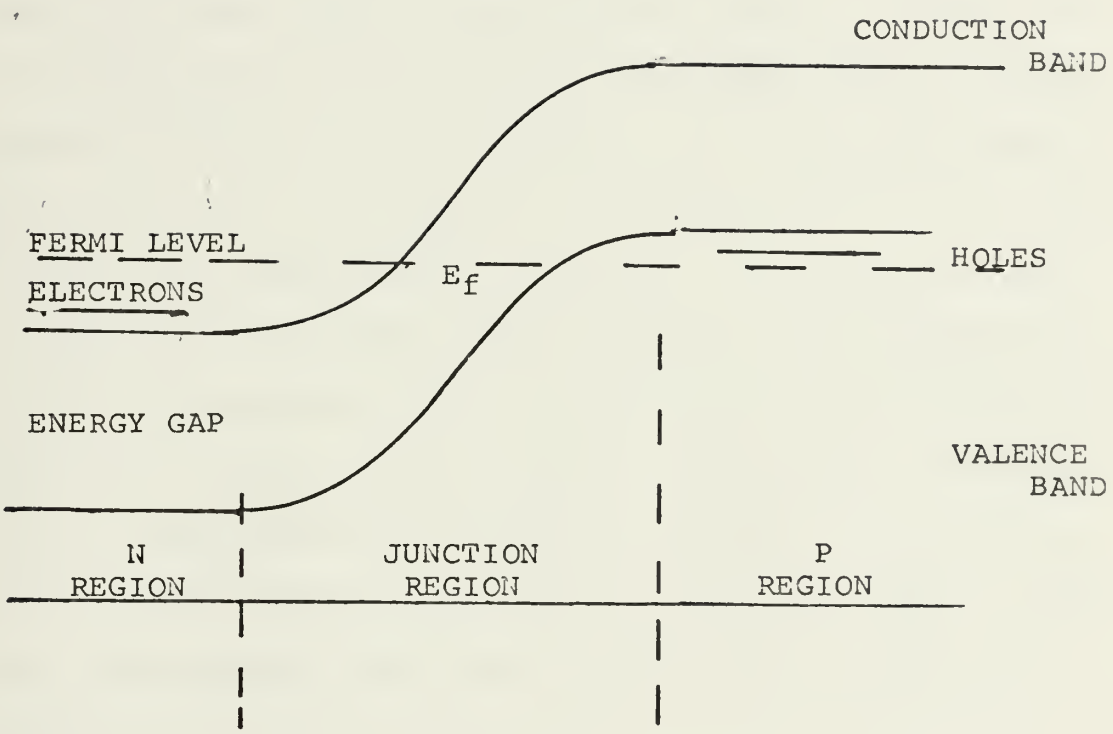

FIGURE 2 ENERGY LEVEL VERSUS DISTANCE ALONG A CROSS SECTION THROUGH A P-N JUNCTION WITH HEAVILY DOPED P AND N REGIONS FOR EQUILIBRIUM WITH NO VOLTAGE APPLIED.

Figure 3 shows the changes that occur when a forward voltage is applied to such a diode. The absolute energy difference, measured in electron volts, between the p and n regions is reduced by the applied potential in volts (the Fermi level is no longer strictly applicable, since the diode is not in equilibrium). It is now possible for both electrons from the n region and holes from the p region to move into the junction region from opposite sides and overlap in at least part of the junction region. In the overlap region, where both electrons and holes are present, it becomes possible for an electron in the conduction band to drop into and fill a vacancy, or hole, in the valence band. The hole and electron then recombine. The excess energy of the electron in this process may go into excitation of acoustic vibrations, which simply heat the surrounding semiconductor crystal lattice (called non-radiative recombination or spontaneous emission of a phonon), or it may go into the spontaneous emission of a photon of light or very near the band-gap wavelength. This light is called the recombination radiation.

Because the probabilities of either nonradiative or radiative recombination are always rather large, neither electrons nor holes can spill very far outside their respective regions before such recombination occurs. Thus the recombination region is limited to a thin layer in the immediate vicinity of the junction (this region is biased somewhat to the p side of Figure 3 because a heavier doping on the n side than the p side was assumed as is often the

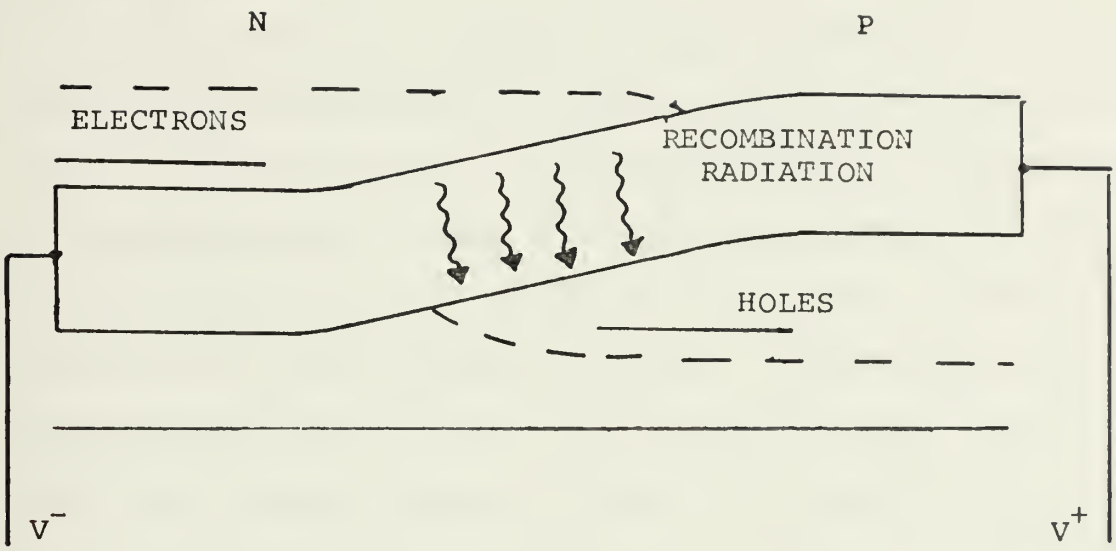

FIGURE 3 ENERGY LEVELS VERSUS DISTANCE ALONG A CROSS SECTION THROUGH A P-N JUNCTION WITH HEAVILY DOPED P AND N REGIONS WITH A FORWARD VOLTAGE APPLIED TO CAUSE CURRENT FLOW AND RADIATIVE RECOMBINATION EMISSIONS.

case in practical Ga As devices). There is, of course, an associated forward current flow through the diode (positive current moving from right to left) because positive hole flow to the left in the p region and negative electrons flow to the right in the n region. These carriers then recombine and annihilate each other in the overlap region of the junction.

If the radiative (light emitting) recombination rate dominates the nonradiative (photon-emitting) recombination rate, as can be the case in optimum materials (direct-band-gap semiconductors), then very nearly one photon of recombination radiation will be emitted for every electron of charge that flows through the diode. If the band-gap of the semiconductor in volts is V_g (typically $V_g \sim .1$ to 1^V), then every emitted photon carriers away energy $e \cdot V_g$. The power supply energy required to send one electron through the diode is $e \cdot V_d$, where V_d is the voltage drop across the diode. This voltage drop will be slightly larger than V_g and will also include contributions due to (ohmic) voltage drops across the p and n regions of the diode and in the diode leads. Thus the energy efficiency of the radiative-recombination process will be

$$\frac{\text{Light-energy Output}}{\text{Electric-energy Output}} = \frac{\text{radiative recombination rate}}{\text{total recombination rate}} \times \frac{V_g}{V_d}.$$

The first factor on the right is sometimes called the internal radiative quantum efficiency. The important point is that in optimum situations both of the right hand factors can approach unity, and the energy efficiency can thus approach 100

percent. An additional consideration is that the p- and n- type regions surrounding the junction region are highly absorbing for the emitted radiation, and in the below-threshold, or nonlaser case only about 10 percent of the radiated light may be able to escape from the semiconductor sample without being internally reflected and reabsorbed. Even so, this process can furnish an extremely efficient and bright narrow-band infrared light source.

Laser action will also occur in the overlap region near the diode junction when the current flow through the diode becomes sufficiently large and exceeds a certain threshold value. When electrons from the n side and holes from the p side are injected into the junction region at a sufficiently high rate, an electron-population inversion is created between filled levels near the bottom of the conduction band and the empty levels (holes) near the top of the valence band. Laser action near the band-edge wavelength then occurs in this thin layer, and laser oscillations can build up between the reflecting ends of the semiconductor sample as shown in Figure 1. If the forward current is increased to a few times the threshold value, virtually all the injected current goes into the laser oscillation. Thus the oscillation output compared to the electrical-energy input can have the same near 100 percent efficiency characteristic of the below threshold recombination radiation described above. The p and n regions surrounding the junction layer are still lossy to the laser

wavelength, so that the laser action is confined to a very thin planar junction region. However, the laser oscillation waves travel largely in the axial direction along this layer and escape into free space through the ends of the diode. Laser efficiencies exceeding 60 percent are possible in low-temperature diodes, although 10 percent or less is more common for room temperature operation, where the p- and n-region losses have more serious effects.

The physical size of the resulting laser device could hardly be smaller - a tiny semiconductor chip, perhaps, in a transistor package with a window on one end and the pumping requirement is simple - a low voltage d-c current source. Thus the semiconductor laser offers unique advantages of small size, simplicity, and extraordinary high efficiency. It can also be a very inexpensive device, well suited to mass fabrication, and it's output can be directly modulated, even up to gigahertz modulation frequencies, simply by modulating the pumping current through the diode. However, this type of laser has some compensating disadvantages. Because of the extreme thinness and generally small size of the laser region, as well as transient heating and other effects that occur during laser action, it is very difficult to control the mode pattern and mode structure of the laser action. The laser beam emerges in a rather wide beam, perhaps 5° to 15°. This beam can be much more narrowly collimated by passing it through a small telescope, but not to nearly the degree possible with, say, gas lasers (although it still far exceeds the capabilities of ordinary

non laser light sources. The laser action in the semiconductor laser originates, not between two sharp and well defined energy levels, but between the edges of two broad bands. Partially as a result of this, the spectral purity and monochromaticity of the injection-laser output is also much poorer than in other types of lasers (although, again, it is still much better than any incoherent light source).

Gallium arsenide provided the first successful semiconductor in late 1962, with successful experiments reported nearly simultaneously by three independent research groups at the General Electric and IBM research laboratories and at MIT Lincoln Laboratory. Gallium arsenide with a band-gap energy of 1.4 to 1.5 eV and a transition wavelength λ = 8400 to 9100 A° (depending upon temperature), is still the most widely used diode laser system, although a half dozen other semiconductors have since been widely made to operate as diode lasers, and many additional materials will exhibit laser action under high-voltage electron-beam excitation. The near infrared transition wavelengths from Ga As can be shifted down to as short as ~ 6500 A° in the visible-red spectrum by employing a mixed semiconductor alloy of Ga As and Ga P, although at some cost in performance. Efficient radiative recombination, as well as diode laser action, appear to be possible in semiconductors having what is known as a direct-gap energy-band structure. As a result, the semiconductors most widely employed is conventional electronic devices, silicon and germanium, are not suitable for

diode laser action, since they are indirect-gap semiconductors [Ref. 3].

E. THE SILICON PHOTODIODE

The silicon photodiode performs the function of collecting the transmitted light signal and converting this signal to frequency varying waveforms. The silicon diode selected was incorporates an operational amplifier to improve the sensitivity characteristics of the detector.

The three principal characteristics of silicon photodiodes that have brought them into recent usage are:

1. Linearity of output power signal current with input light power level changes.

2. A wide light level detection capability using the new PIN construction.

3. Excellent long term stability [Ref. 4].

A PIN photodiode is one in which a heavily doped P region and a heavily doped N region are separated by a lightly doped "i" region. This "i" region resistivity can range from 10 ohm cm to 100,000 ohm cm, the p and n regions being less than 1 ohm cm. The output from this two terminal sensor is a current whose value is proportional to the input light power. A Planar Diffused PIN photodiode is shown in Figure 4(a).

These photodiode structures can be operated photo-conductively, i.e., in a current mode or photovoltaically, i.e., in a voltage mode. For speed and linearity of response, the current mode is preferred [Ref. 4].

The minimum energy of a photon required for intrinsic excitation is the forbidden-gap energy E_g (electron volts) of the semiconductor material. The wavelength λ_c of a photon whose energy corresponds to E_g is given by

$$\lambda_c = \frac{1.24}{E_g}$$

where λ_c is expressed in microns and E_g in electron volts. If the wavelength of the radiation exceeds λ_c, then the energy of the photon is less than E_g and such a photon cannot cause a valence electron to enter the conduction band. Hence λ_c is called the critical, or cutoff wavelength or long wavelength threshold of the material.

The spectral-sensitivity curves for S_i and G_e are plotted in Figure 4(b) indicating that a photoconductor is a frequency-selective device.

If a forward bias is applied, the potential barrier is lowered and the majority current increases rapidly. When this majority current equals the minority current, the total current is reduced to zero. This voltage at which zero resultant current is obtained is called the photovoltaic potential.

Consider the p-n junction of Figure 5(a) illuminated with photons of greater-than-gap energy. The absorption of the photon results in the creation of a hole-electron pair. The "built-in" field at the junction drives the two carriers in opposite directions; the electron to the n-type region, the hole to the p-type region. The charge separation results in a potential difference V across the junction

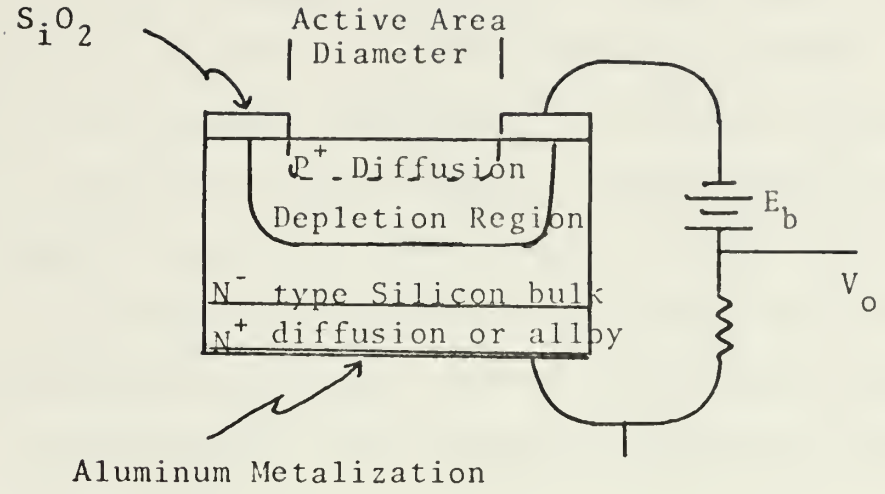

FIGURE 4(a) PIN PHOTODIODE DIAGRAM.

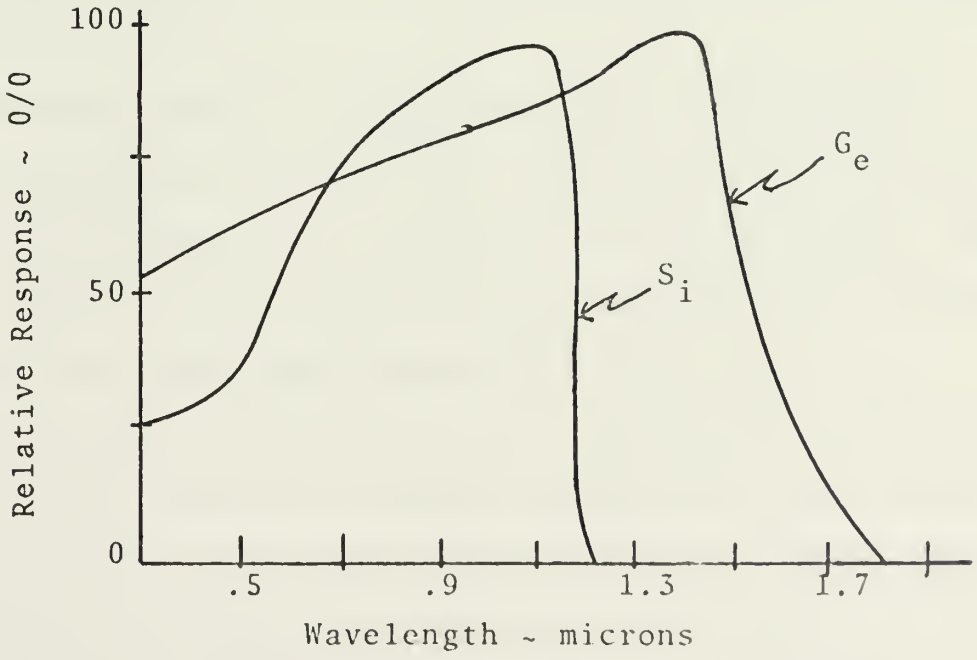

FIGURE 4(b) SPECTRAL RESPONSE OF S_i and G_e.

as in Figure 5(b). Note that in this process the carriers have become majority carriers and, therefore, are endowed with an infinite lifetime. However, the potential difference set up by the photo-generated, field-separated pair biases the p-n junction in the forward direction. Hence some of the carriers, overcoming the lowered barrier ϕ_b-qV, will be injected into the opposite region, where they become minority carriers and recombine. If an external circuit is connected across the p-n junction, one can measure the photovoltaic voltage V or, if the load resistance is low, a photocurrent, the illuminated junction acting as a battery. [Ref. 5].

F. THE ATMOSPHERIC TRANSMISSION MEDIUM

In as much as the interest in short-range line-of-sight laser communication systems is high, it is noteworthy to mention the transmission characteristics of the space medium as related to lasers.

The signal quality of a system across a link can be severly degraded by snow or fog, indicating that 100% availability is possible only if very short links are used. The extent to which less availability is acceptable must be decided for each individual system [Ref. 6].

Transmission degradation in the atmosphere is caused by the scattering losses for visible and near infrared signals. If the fog were sufficiently thick enough, the energy beam would diffuse outward in all directions and a highly directional beam would be reduced to an isotropic radiator. If

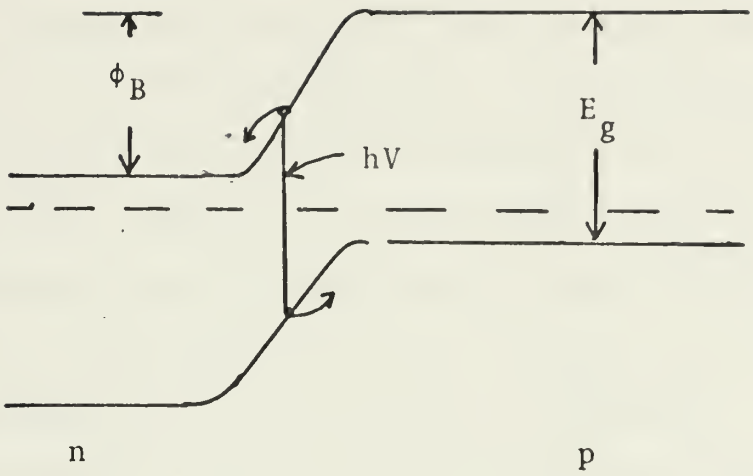

FIGURE 5(a) P-N JUNCTION AT PHOTON ILLUMINATION

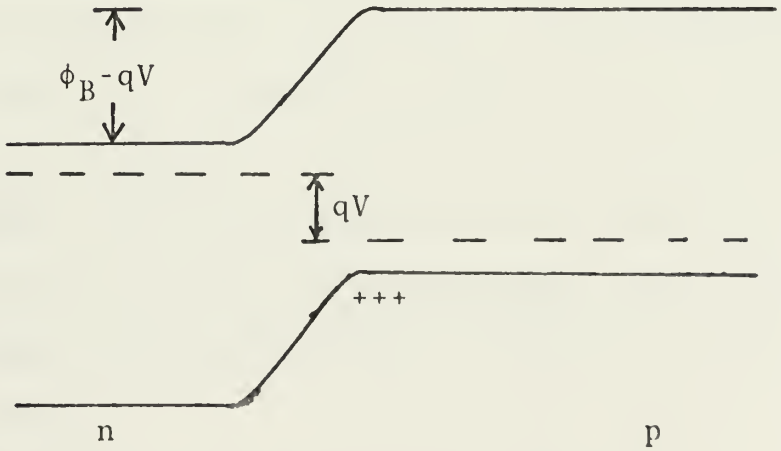

FIGURE 5(b) GENERATION OF PHOTOVOLTAIC VOLTAGE V

sufficient power were available to overcome these losses, the beam would propagate equally in all directions and any security afforded by the directionality of the system would be lost. This scattering is of two principal types, Mie scattering and Rayleigh scattering. Rayleigh scattering is directly proportional to the wavelength and is relatively unimportant for wavelengths longer than 1 micron. It is only important when the particles are small with respect to wavelength. For larger particles, the Rayleigh scattering is insignificant and Mie scattering is dominant. As Mie scattering becomes dominant, the scattering becomes independent of wavelength. Beam broadening and beam wondering due to turbulence in clear air should also be considered as a possible serious problem. Another potentially serious problem with any optical communications system is that of scintillation introduced by atmospheric turbulence.

Attenuation in the atmosphere is mainly due to the presence of water vapors and carbon dioxide in the atmosphere. There are three spectral intervals called "atmospheric windows" which for acceptable transmissivity. They are located at 0-2.5 microns, 3-5 microns, and 8-13 microns. These windows and absorbing mediums are shown in Figure 6. In the infrared portion of the spectrum, the absorption process poses a far more serious problem than does the scattering process.

Figure 7 shows the approximate variation of the attenuation coefficients with wavelength at sea level for various

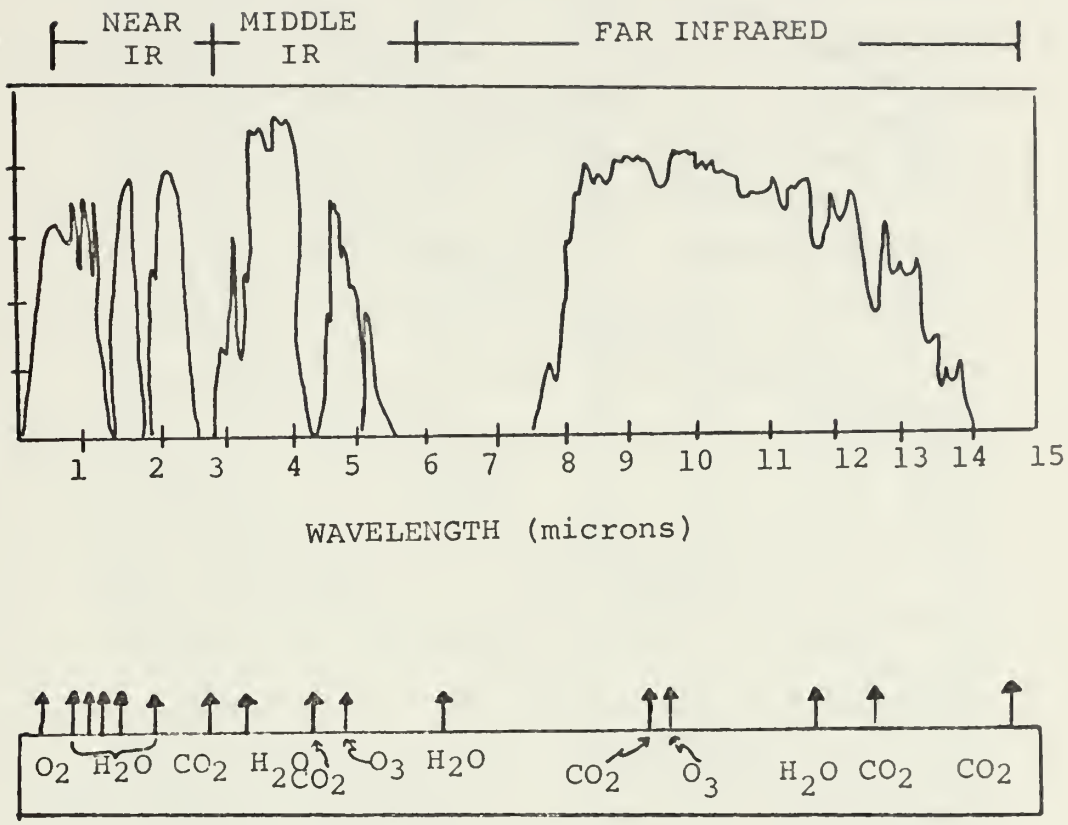

FIGURE 6 TRANSMITTANCE OF THE ATMOSPHERE FOR A 6000 FT HORIZONTAL PATH AT SEA LEVEL.

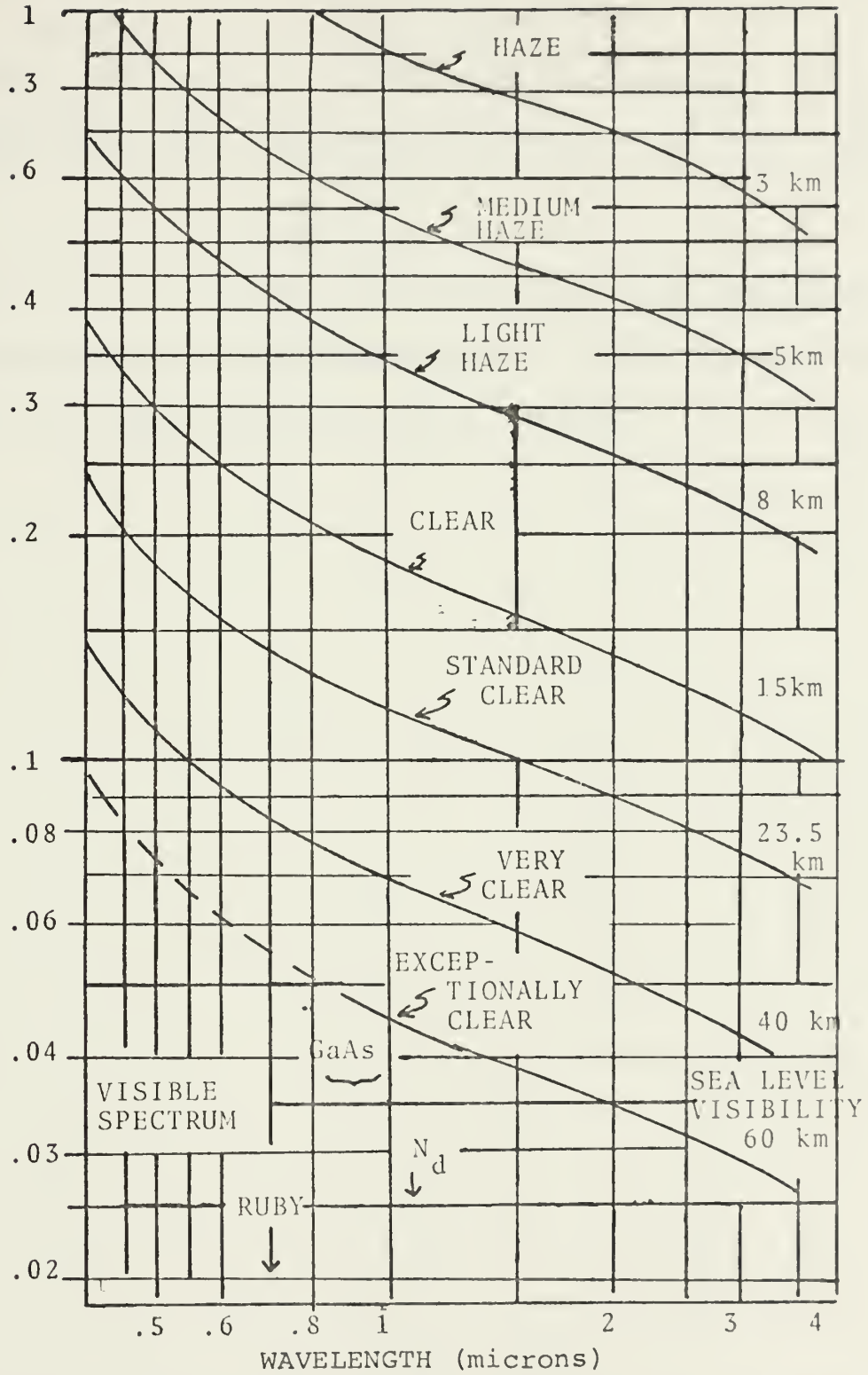

FIGURE 7 APPROXIMATE VARIATION OF ATTENUATION COEFFICIENT WITH λ AT SEA LEVEL FOR VARIOUS ATMOSPHERIC CONDITIONS.

atmospheric conditions while neglecting absorption by H_2O vapor and CO_2.

The transmittance of the signal is a function of both the absorption and scattering coefficients as shown below,

$$T = e^{-\sigma x}$$

where $\sigma = a + \gamma$, a being the absorption coefficient and γ is the scattering coefficient while x is the distance over which the signal is being transmitted [Ref. 7].

III. PROPOSED DESIGN

A. TRANSMITTER DESIGN

The transmitter as described earlier is shown in Figure 8. The input microphone was a high impedance type with a frequency response in the 100-8000 Hz frequency range.

As it was necessary to limit the frequency range to 3000 Hz and to amplify the output signal from the microphone, a high gain notch filter was selected to perform both functions. The principle speech information in the audio range lies between 300-700 Hz so linearity in this area was important.

The audio pre-amplifier/notch filter designed made use of operational amplifier circuit techniques. The actual design of the circuit is quite similar to the notch filter utilized in the receiver with modifications to improve the gain and to impedance match the high impedance, 50 kilo-ohms, of the input microphone. The gain vs. frequency plot is shown in Figure 9. The gain modification was achieved through variation of the feedback RC network while the impedance match was achieved by modifying the input circuit to account for the 50 Kohm microphone impedance. The resulting circuit exhibited 17 db of attenuation at the 3000 Hz point of interest while maintaining a relatively flat response across the desired bandwidth.

While varying the gain of the feedback network, it was also necessary to maintain the frequency selectivity

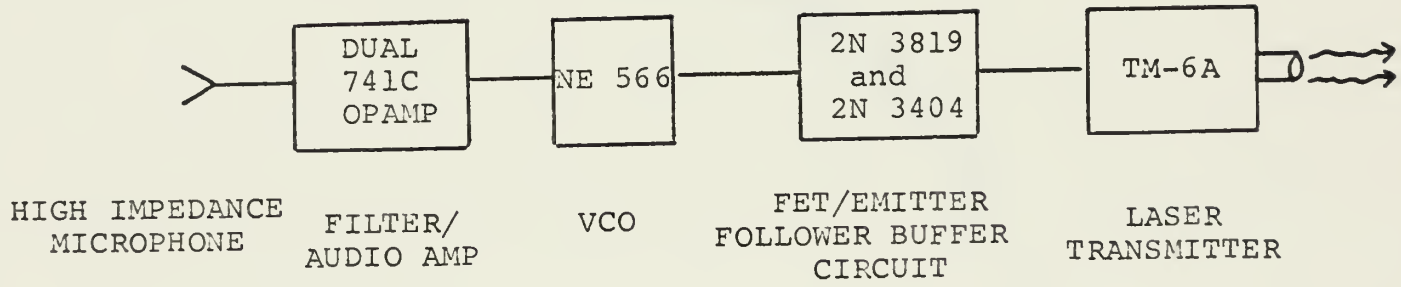

FIGURE 8 TRANSMITTER BLOCK DIAGRAM

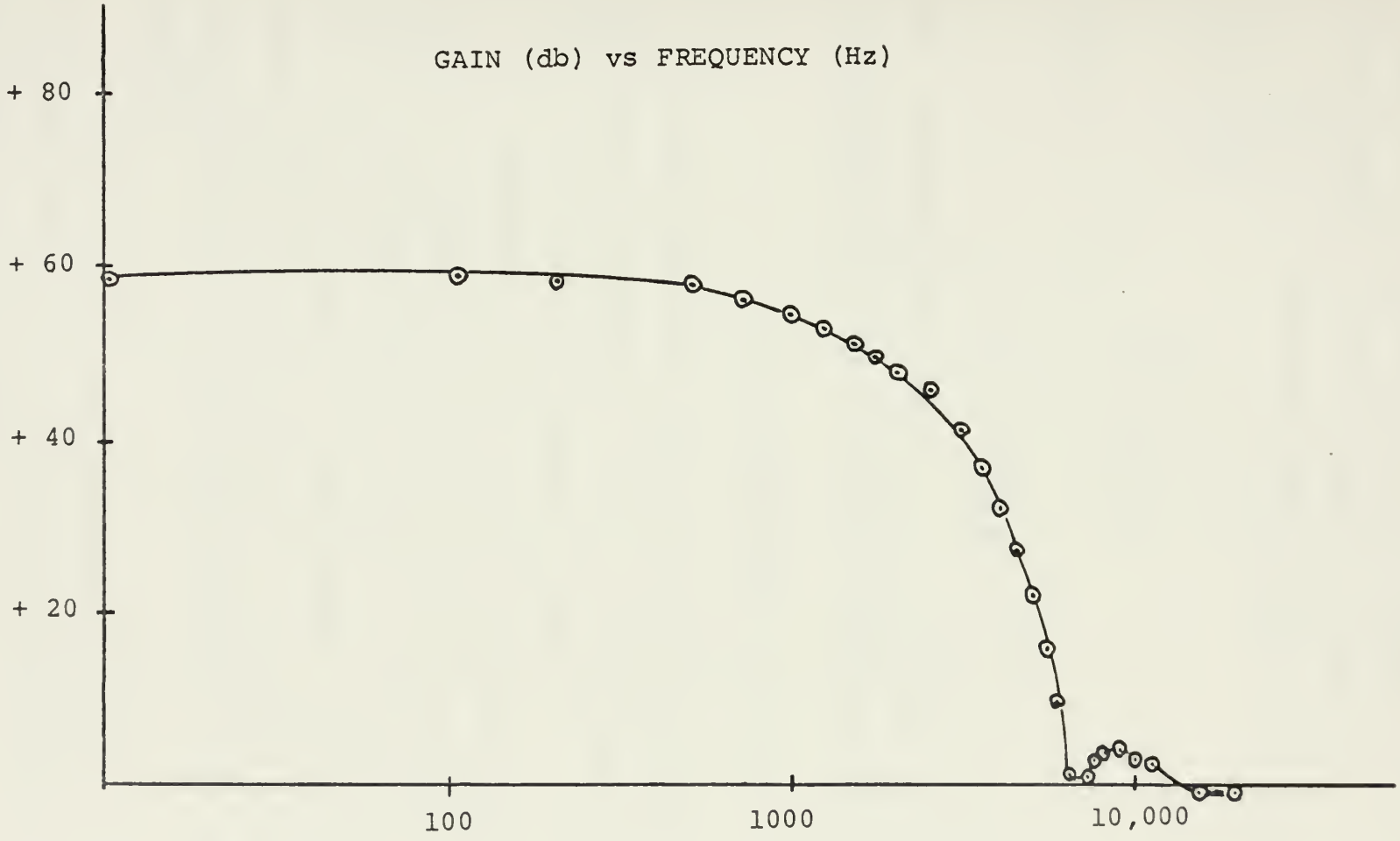

FIGURE 9 AUDIO PRE-AMP FREQUENCY RESPONSE

characteristics of the filter. This required corresponding capacitor variations as well as feedback resistor changes. The completed circuit is shown in Figure 10.

Gain is a function of the feedback resistance as expressed by

$$\frac{E_o}{E_i} = y_{21} R_f$$

where

$$y_{21} = \frac{1}{4.23 K} .$$

For a gain of about 500, R_f is on the order of 1.0 megohms. To maintain the desired frequency characteristics,

$$C_f = \frac{2.28 \times 10^{-5}}{1.0 \times 10^6} = 22 \text{ pfd.}$$

The gain could have been raised in the second stage of the circuit if desired by using similar computations to arrive at the necessary component values.

The modulation scheme to be utilized made use of a commercially available Voltage Controlled Oscillator (VCO). The VCO displayed excellent stability and the linearity of the square wave output was exceptional. The frequency of the oscillation was determined by an external resistor and capacitor as well as the voltage applied to the input terminal.

A typical circuit configuration is shown in Figure 11. The control terminal (pin 5) must be biased externally with a voltage (V_c) in the range

$$3/4 \ V^+ \leq V_c \leq V^+$$

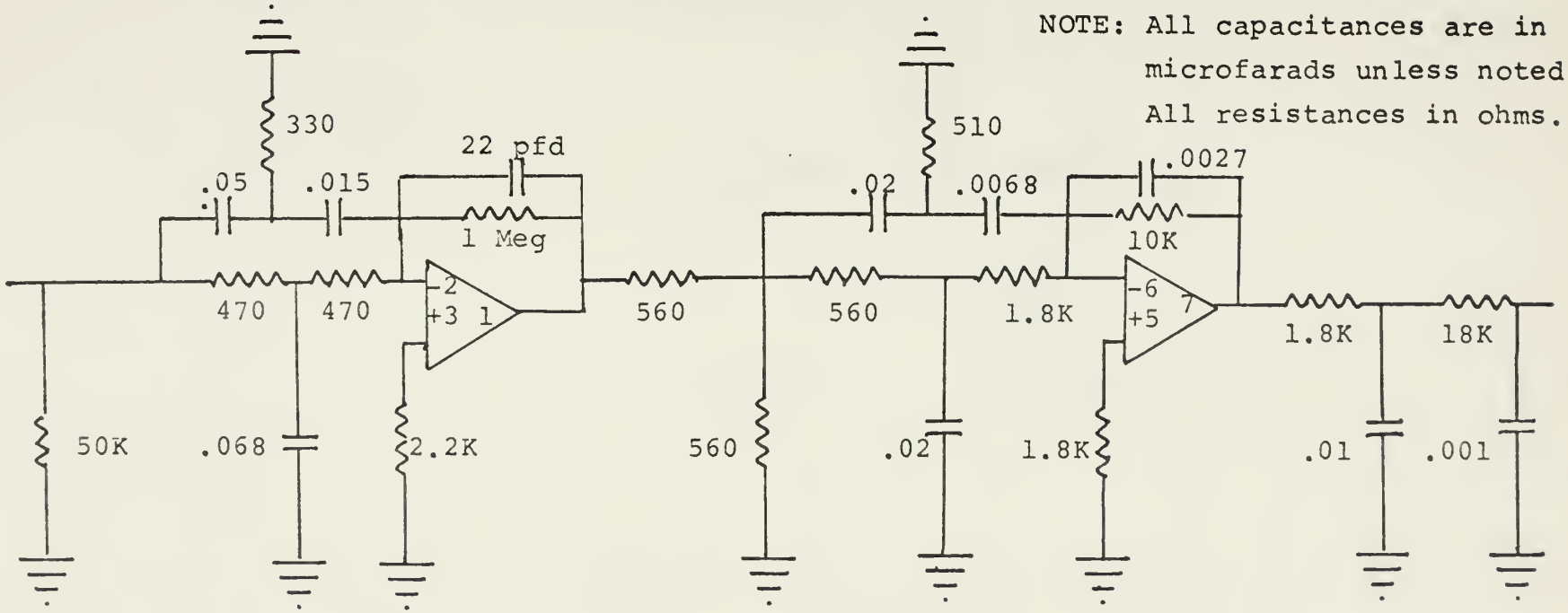

FIGURE 10 AUDIO PRE-AMPLIFIER/NOTCH FILTER

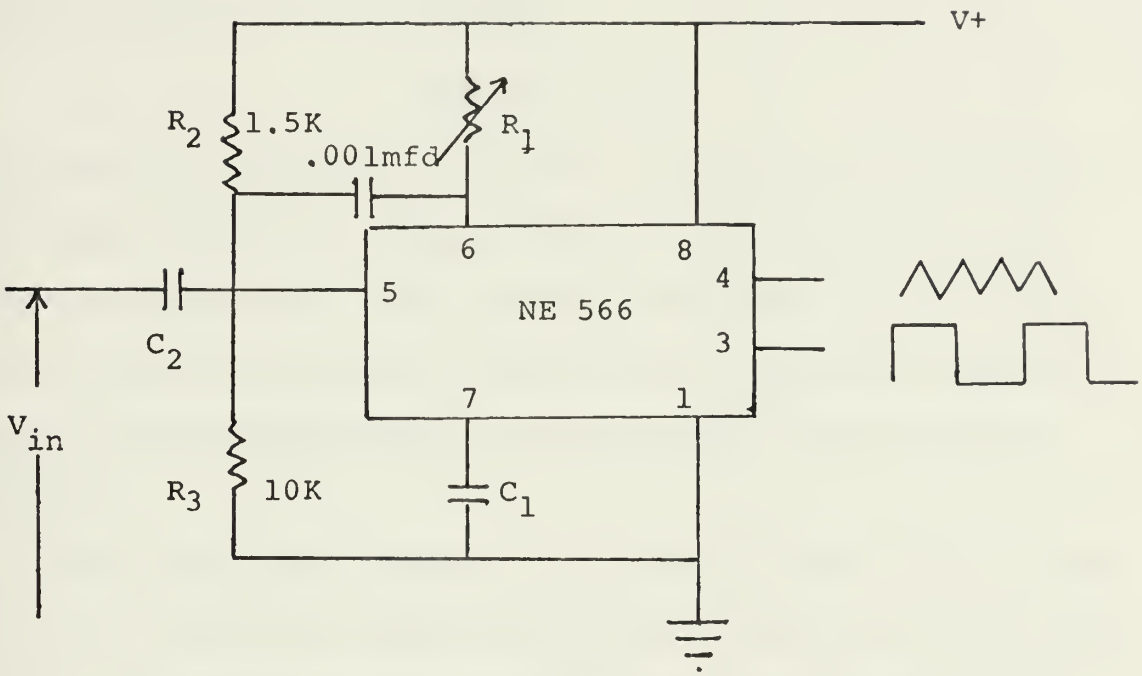

FIGURE 11 A TYPICAL VCO CIRCUIT CONFIGURATION

where V^+ is the total supply voltage. The control voltage is set by the voltage divider formed by R_2 and R_3. The modulating signal is coupled with the capacitor C_2. The oscillating frequency is given approximately by

$$f_o = \frac{2(V^+ - V_c)}{R_1 C_1 V^+}$$

and R_1 should be in the range

$$2\ K \leq R_1 \leq 20\ Kohm.$$

To allow for variation in supply voltages and to minimize component variation problems, R_1 was selected to be a 25 Kohm potentiometer. This allowed the power supply voltage to be varied as desired without actual replacement of components while maintaining the appropriate 7 kHz carrier frequency.

The square wave output was extremely linear with a typical rise time of 20 nanoseconds while maintaining a 50% duty cycle. The square wave output of the VCO is shown below.

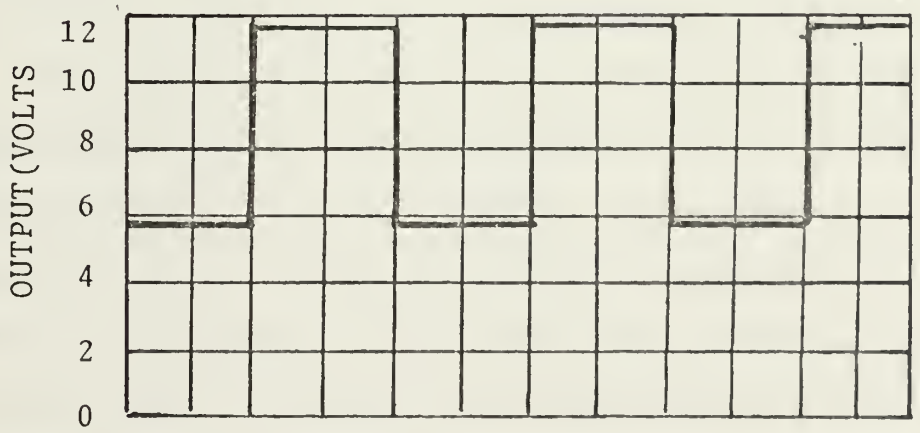

The transfer characteristics of the VCO are shown in Figure 12. Although these characteristics were obtained for a power supply voltage of 15^{volts}, the results are quite similar when a 9^{volt} supply voltage is used.

The laser transmitter, a TM6A, manufactured by the Electronics Products for Industry Corporation, transmitted infrared light in the .905 micron region with a peak power of up to 6 watts and an optical pulse width of approximately 7 nanoseconds and rise times of less than 1 nanosecond. A maximum pulse repetition rate of 10 kHz was obtainable with the above characteristics. Theoretical ranges of greater than one mile in dust and haze conditions was predicted. The colliminating lens concentrates the energy in a narrow beam to enhance the range of the transmitter.

The laser transmitter utilized incorporated the triggering circuit as well as the Ga As laser diode. The trigger circuit, assumed to be of the Schmitt trigger design, required that the input pulse have a maximum rise time of less than .1 microsecond and a minimum of 3^{volts} and a maximum of 6^{volts} amplitude for proper lasing operation.

The input impedance was reported to be 50 ohms which would have been an ideal impedance match with the output resistance of the VCO. However, the transmitter, when coupled to the VCO, would adversely load the VCO and completely distorted the VCO square wave output pulse. Also insufficient information was available to determine the affect that the negative going pulse, which was obtained

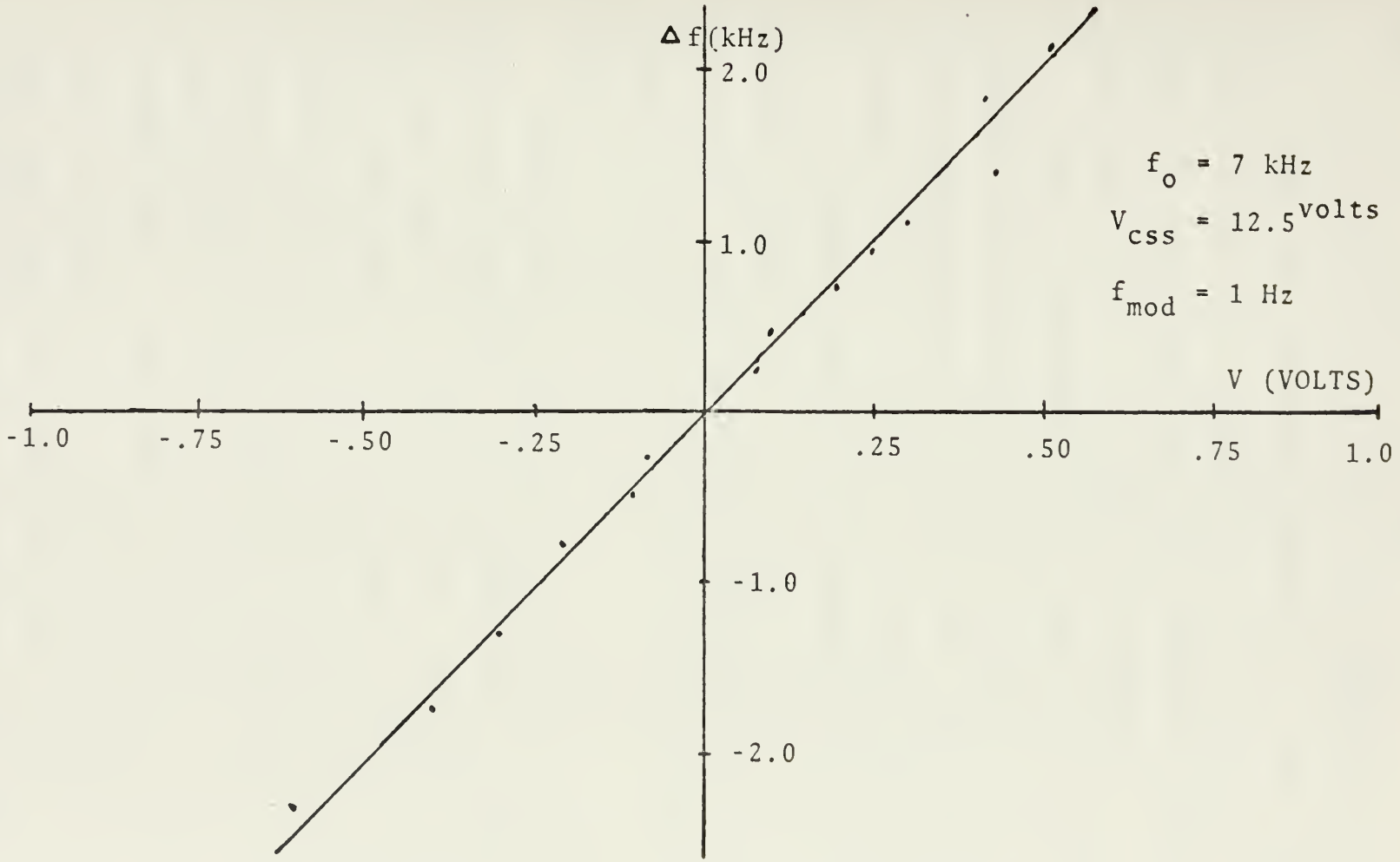

FIGURE 12 VCO TRANSFER CHARACTERISTICS.

by A-C coupling the VCO output to the transmitter, would have on the triggering circuitry.

Several buffering circuits were considered to solve both of the above mentioned problems. A simple diode rectifier circuit was considered but the linearity of this device was questionable and later laboratory experiments proved this device to be highly unacceptable.

In order to maintain the required linearity while clamping the waveform to ground potential, a FET common source configuration was decided upon. The clamping function was obtained by biasing the FET near the cutoff point so as to cutoff current flow through the device during the negative swing of the output signal of the VCO. The circuit used a 2N 3819 transistor whose transfer characteristics were obtained on a Tektronic type 576 transistor curve tracer.

To maintain the linearity, the FET was used in the region beyond pinch-off, the voltage where I_d begins to level off and approach a constant value. In order to bias near the cutoff point, it was necessary to reverse bias the gate junction with a V_{gs}, the voltage between the gate and the source, of sufficient magnitude to narrow the conduction channel width so that I_{ds}, the drain to source current, approaches zero. Under these conditions, any further reverse bias of the gate, i.e., any negative voltage applied to the gate, will cause the transistor to be further biased into the cutoff region while any positive going pulse on the gate will cause the transistor to conduct.

The circuit of Figure 13(a) was utilized to successfully obtain the desired operating point. While this circuit maintained the linear waveform characteristics and pulse shape desired, it was also loaded down by the transmitter circuitry. An emitter follower bipolar transistor configuration was used as the final stage of the buffer circuit. The emitter follower configuration is characterized by a high input impedance, typically on the order of 144 K ohms, and a low output impedance on the order of tens of ohms. The configuration also exhibits near unity gain while increasing the power level of the signal. The designed circuit utilized a 2N 3404 transistor in the configuration shown in Figure 13(b). Figure 14 shows the completed buffer circuit and the associated waveforms. The circuit maintained the required linear pulse output when coupled to the transmitter circuitry.

The completed transmitter is shown in Figure 25(a). The TM-6A is mounted on the top of the modulation circuitry with the 200^{volt} d-c power supply input on the side of the chassis. Provisions for mounting a telescope, for alignment of the transmitter lens with the detector window, were made with the telescope mounting located on the side of the transmitter.

The fact that the TM-6A transmitter required a supply voltage of between 160 to 200^{volts} d-c is the limiting factor in the portability of the system. For an operational system, it would be highly desirable to use a pulser/laser

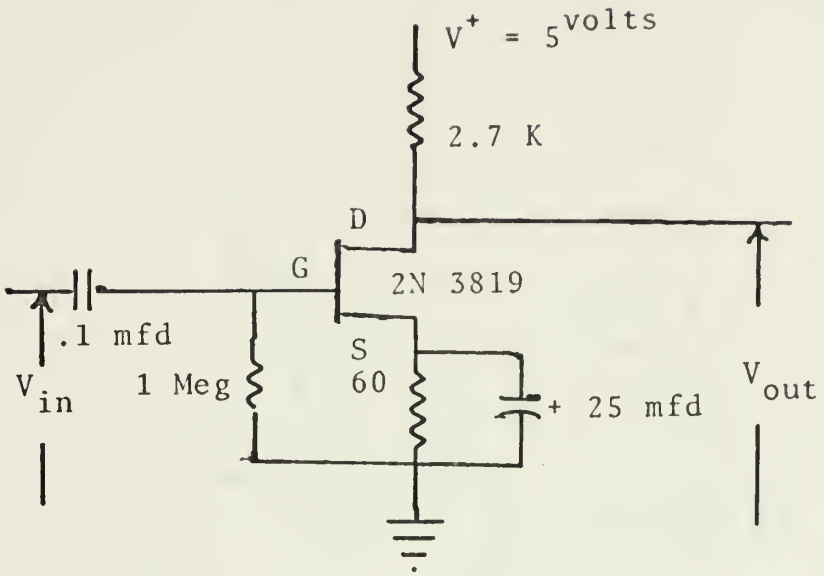

FIGURE 13(a) FET CIRCUIT CONFIGURATION

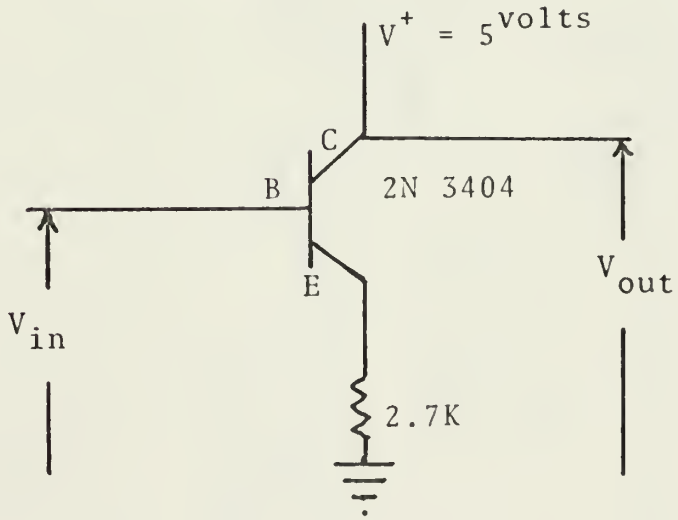

FIGURE 13(b) EMITTER FOLLOWER CIRCUIT CONFIGURATION

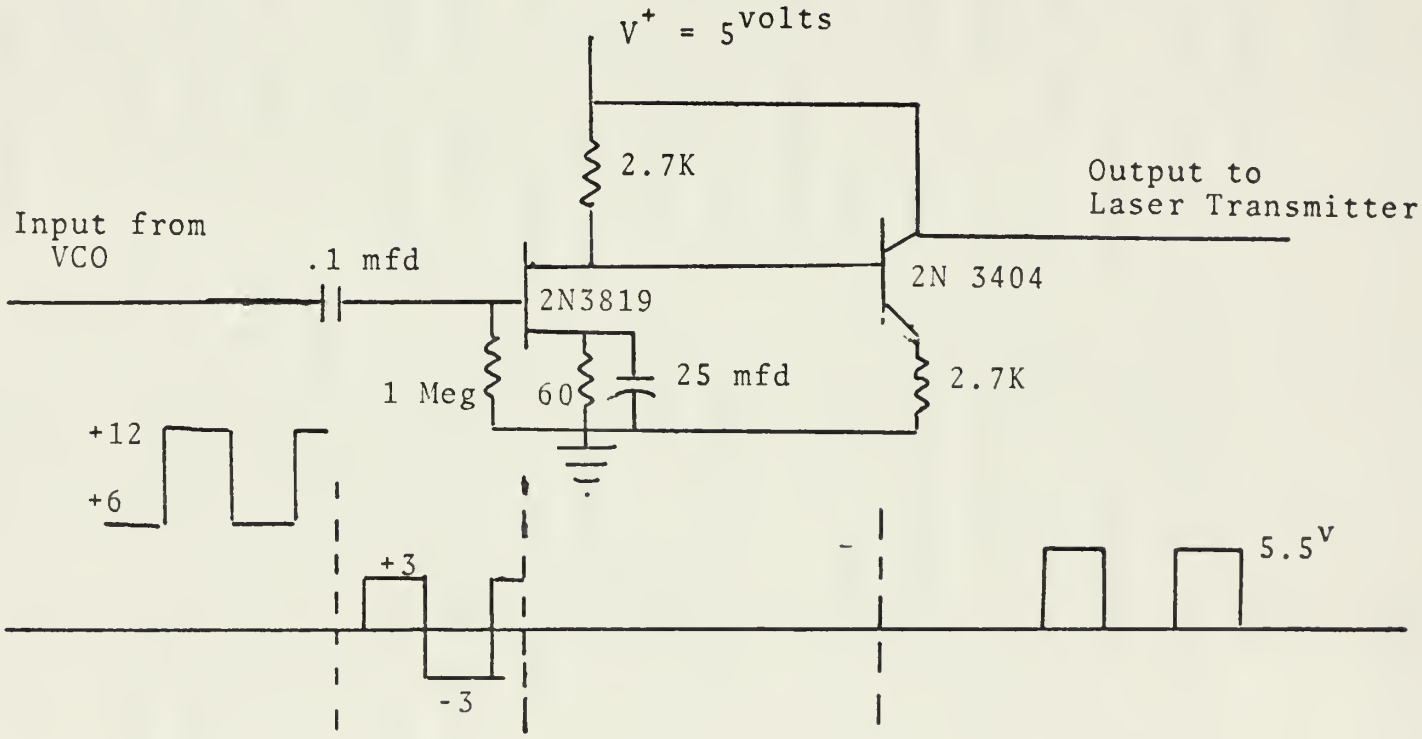

FIGURE 14 BUFFER CIRCUIT AND ASSOCIATED WAVEFORMS

diode combination which would operate from a lower supply voltage, preferably one with a 9^{volt} transistor battery compatability.

B. THE RECEIVER

The block diagram of the proposed receiver is shown in Figure 15. A photodiode detector was used to collect the light information signal and to transform this into electrical energy. The spectral response of the detector is shown in Figure 16(a), as the transmitter emits light in the .905 micron range, the detector responsivity is about 15 millivolts/microwatt.

The FDA 425 detector, packaged as a 14 pin flat pack, utilizes an operational amplifier to attain these response figures. The operation of the photodiode was more fully explained in an earlier section of this thesis. The low single voltage and low input current requirements make this package very compatible with the integrated circuitry used in the receiver. Figure 16(b) shows the circuit configuration used in this application, where R_f is internal to the package while R_1 is utilized as a current limiting resistor. A small capacitor (.01 mfd) is connected between V^+ and ground.

Upon investigating the input requirements of the Phase Locked Loop (PLL), it was determined that the input pulse-widths, on the order of a few nanoseconds, were insufficient at the repetition rates of the system. The PLL requires a 40-50% duty cycle for optimum operation which, at the system

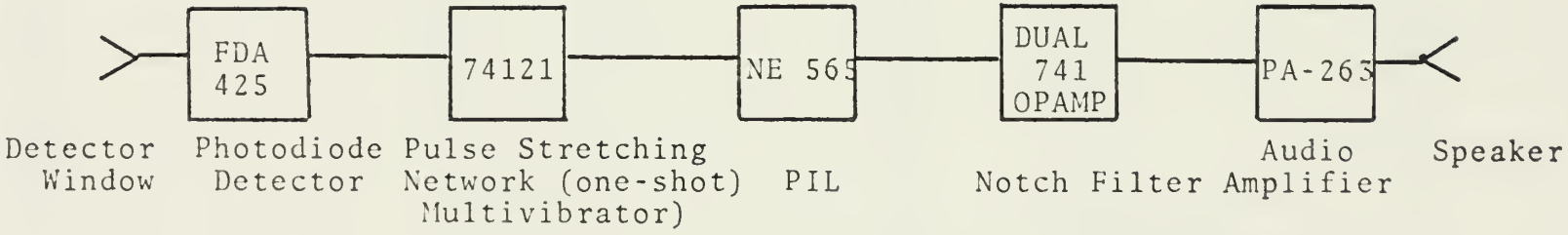

FIGURE 15 RECEIVER BLOCK DIAGRAM

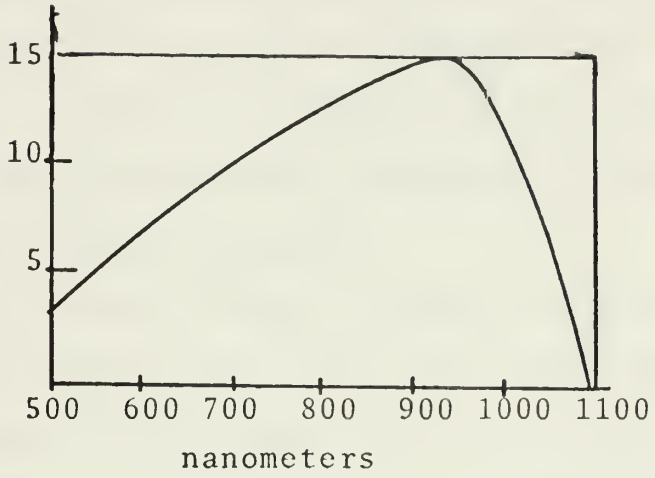

FIGURE 16(a) PHOTODETECTOR SPECTRAL RESPONSE.

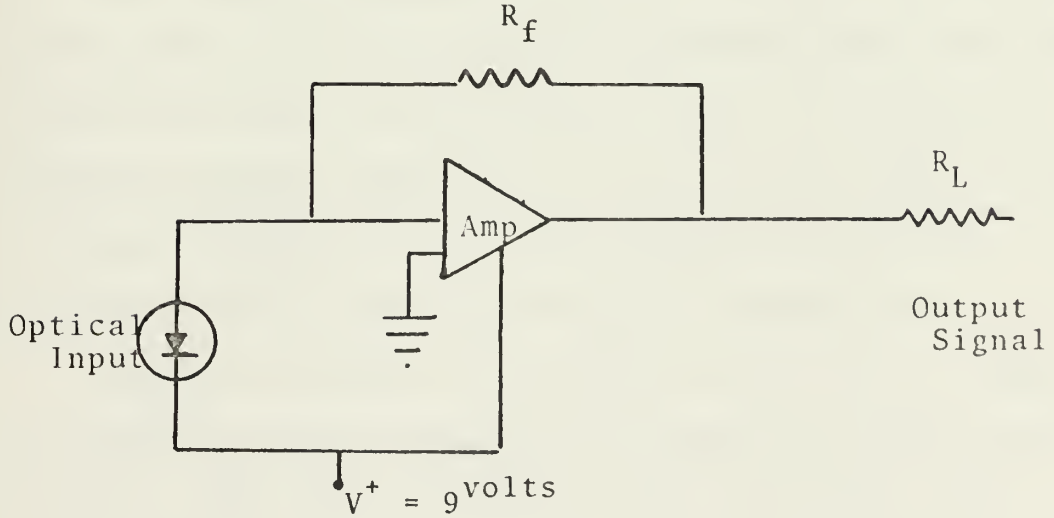

FIGURE 16(b) PHOTODETECTOR CIRCUIT CONFIGURATION.

7 kHz repetition rate, would require pulse widths on the order of .07 milliseconds.

To meet these requirements, it was decided that a mono-stable multi-vibrator would meet the specifications for the pulse stretching network. The particular multi-vibrator chosen, a N 74121 integrated circuit, featured an output pulse length which could be varied by choosing appropriate external timing components.

The circuit utilized, shown in Figure 17, produced a .09 millisecond pulse which was relatively constant over the range of frequencies from 4.5 kHz to 9.5 kHz as evidenced in the photographs of Figure 18. The circuit truth table is shown in Figure 17(b). The output pulse widths are a function of timing components such that;

$$t_p(\text{out}) = C_t\ R_t\ \text{Log}_e\ 2.$$

The circuit triggers on either a positive or negative going pulse of at least 2^{volts} depending upon the trigger inputs utilized. As used here, input B is a positive Schmitt-trigger input for slow edges or for level detection and will trigger the one shot whenever input B goes to a logical 1 with either A_1 or A_2 at a logical 0.

The PLL utilized, a conventional NE 565, is comprised of a VCO, a phase comparator, an amplifier and a low pass filter. The block diagram is shown in Figure 19(a).

The free running frequency of the VCO is determined by

$$f_o = \frac{1}{4R_1C_1} \text{ in Hz}$$

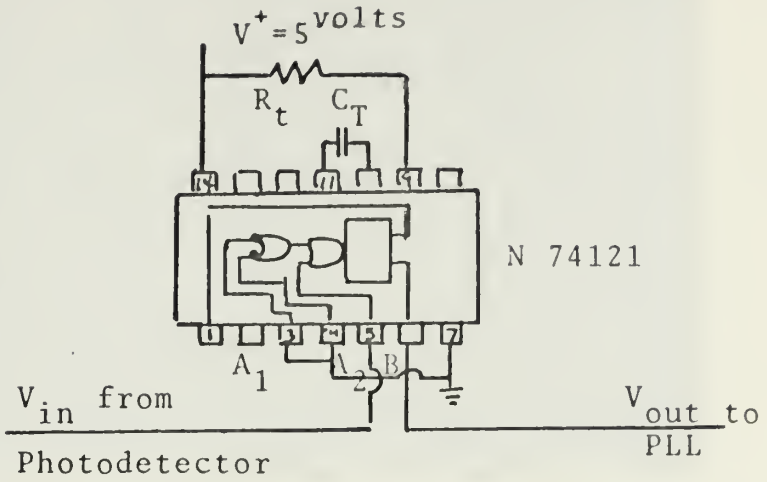

TRUTH TABLE

t_n Input			t_{n+1} Input			Output
A_1	A_2	B	A_1	A_2	B	
1	1	0	1	1	1	INHIBIT
0	x	1	0	x	0	"
x	0	1	x	0	0	"
0	x	0	0	x	1	1shot
x	0	0	x	0	1	"
1	1	1	x	0	1	"
1	1	1	0	x	1	"
x	0	0	x	1	0	INHIBIT
0	x	0	1	x	0	"
x	0	1	1	1	1	"
0	x	1	1	1	1	"
1	1	0	x	0	0	"
1	1	0	0	x	0	"

FIGURE 17 MULTIVIBRATOR CIRCUIT AND TRUTH TABLE.

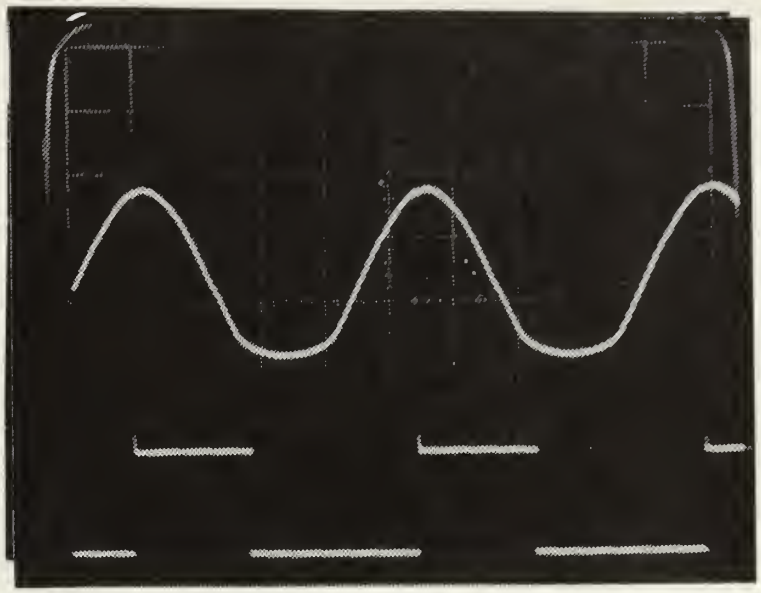

INPUT SINE WAVE---------- 4.5 Khz
HORIZONTAL SCALE--------- 50 microseconds/DIV
VERTICAL SCALE----------- 1 volt/DIV
OUTPUT FREQUENCY-- ------ 4.54 Khz
OUTPUT PULSE WIDTH------- .09 milliseconds

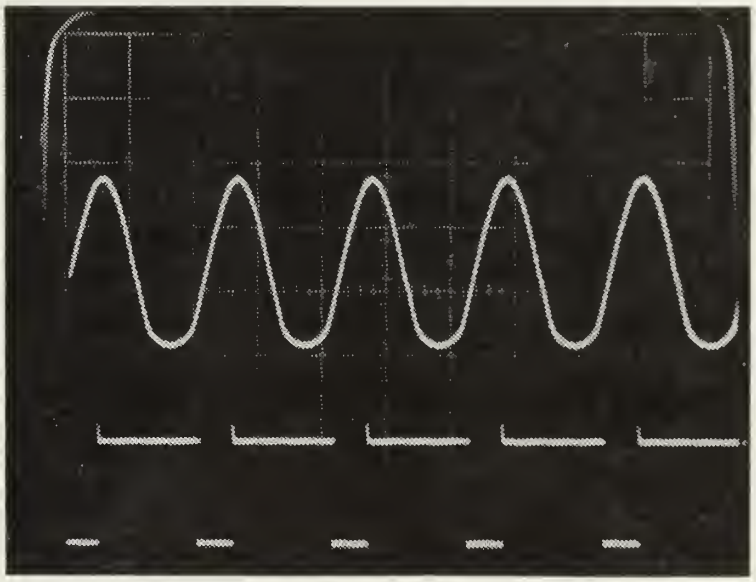

INPUT SINE WAVE---------- 9.5 Khz
HORIZONTAL SCALE--------- 10 microsecond/DIV
VERTICAL SCALE---- ------ 1 volt/DIV
OUTPUT FREQUENCY--- ----- 9.[illegible] Khz
OUTPUT PULSE WIDTH------- .0[illegible] milliseconds

FIGURE 16 INPUT vs OUTPUT OF [illegible] MULTIVIBRATOR

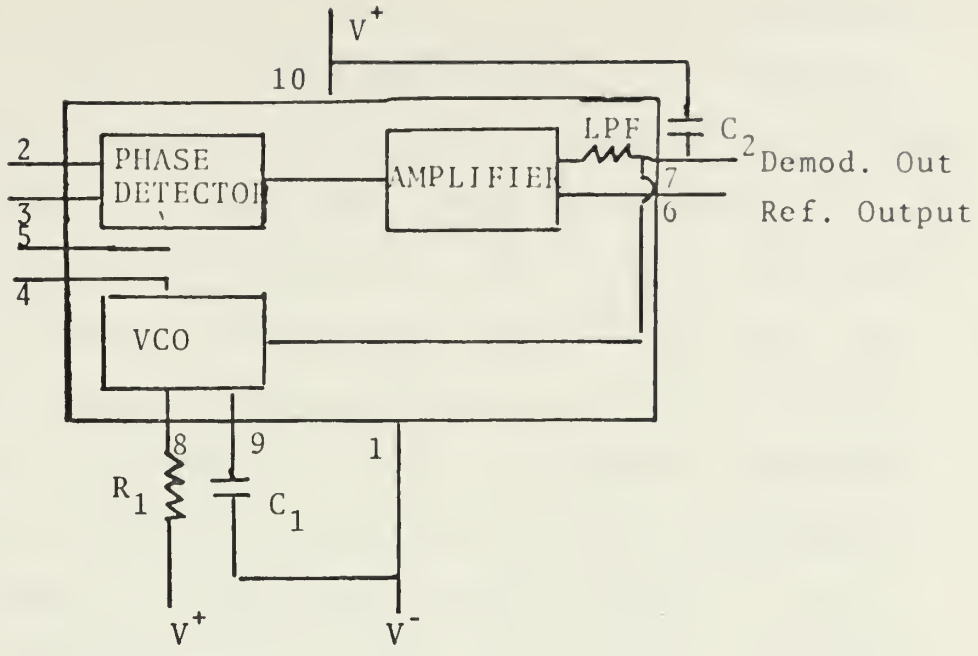

FIGURE 19(a) PLL BLOCK DIAGRAM

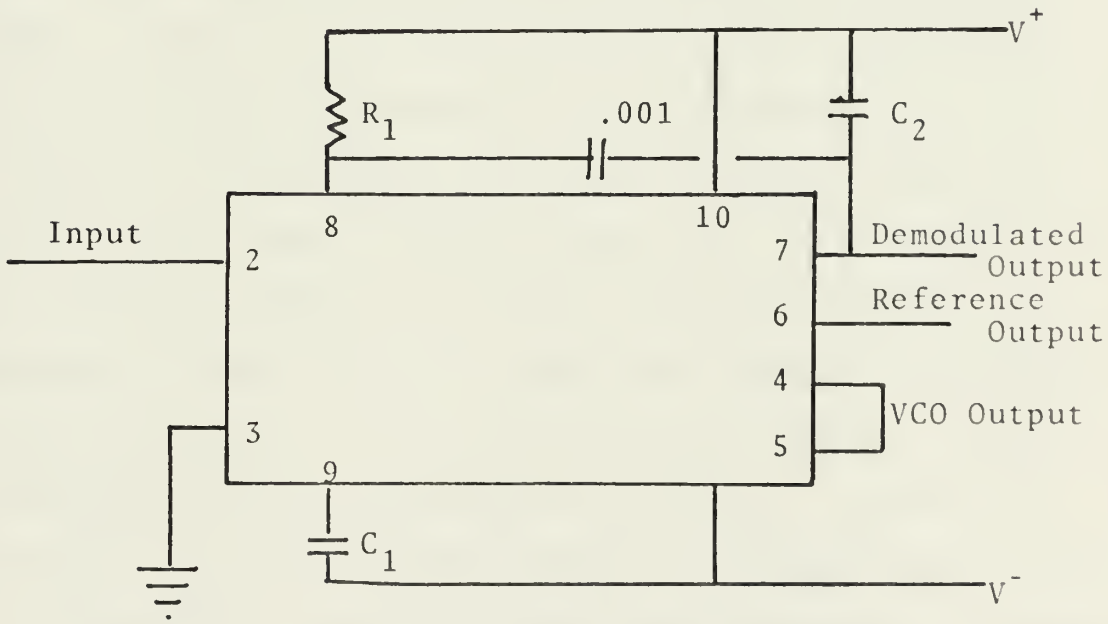

FIGURE 19(b) PLL CIRCUIT CONFIGURATION

and should be adjusted at the center of the input frequency range, i.e., 7 kHz. For this application, C_2 = .015 mfd., C_1 = .01 mfd and R_1 is variable in the range from 2-25 Kohms. To increase the lock range (that range of frequencies in the vicinity of f_o over which the VCO, once locked to the input signal, will remain locked) a $V_{cc} = \pm 9^{volts}$ was used. At this voltage, the PLL would track from 4.2 kHz to 9.5 kHz. During lock, the average d-c level of the phase comparator output signal is directly proportional to the frequency of the input signal. As the input frequency shifts, it is this phase comparator output signal which causes the VCO to shift it's frequency to match that of the input. Consequently, the linearity of the phase comparator output frequency is determined by the voltage transfer function of the VCO. Figure 20 is a plot of the transfer characteristics of the PLL as it was used in this application.

Because of it's unique and highly linear VCO, the PLL can lock to and track an input signal over a very wide range (typically ±60% of f_o) with very high linearity (typically, within 0.5%). A simplified diagram of the VCO is shown in Figure 21. I_1 is the charging current created by the application of the control voltage V_c. In the initial state, T_3 is off and the current I_1 charges the capacitor C_1 through the diode D_2. When the voltage on C_1 reaches the upper triggering threshold, the Schmitt Trigger changes state and turns on the transistor T_3. This provides a current sink and essentially grounds the emitters of T_1 and

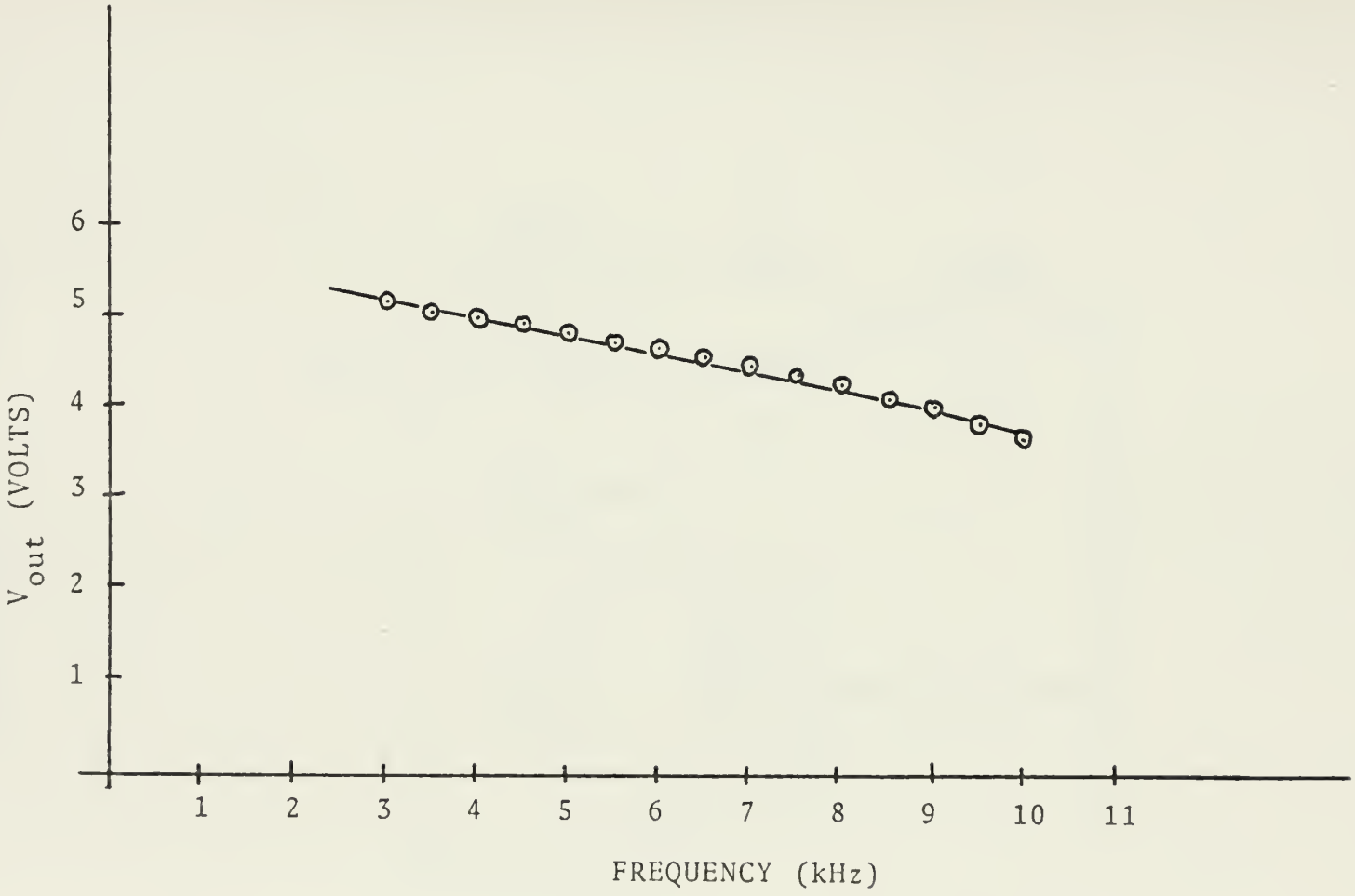

FIGURE 20 PLL TRANSFER CHARACTERISTICS

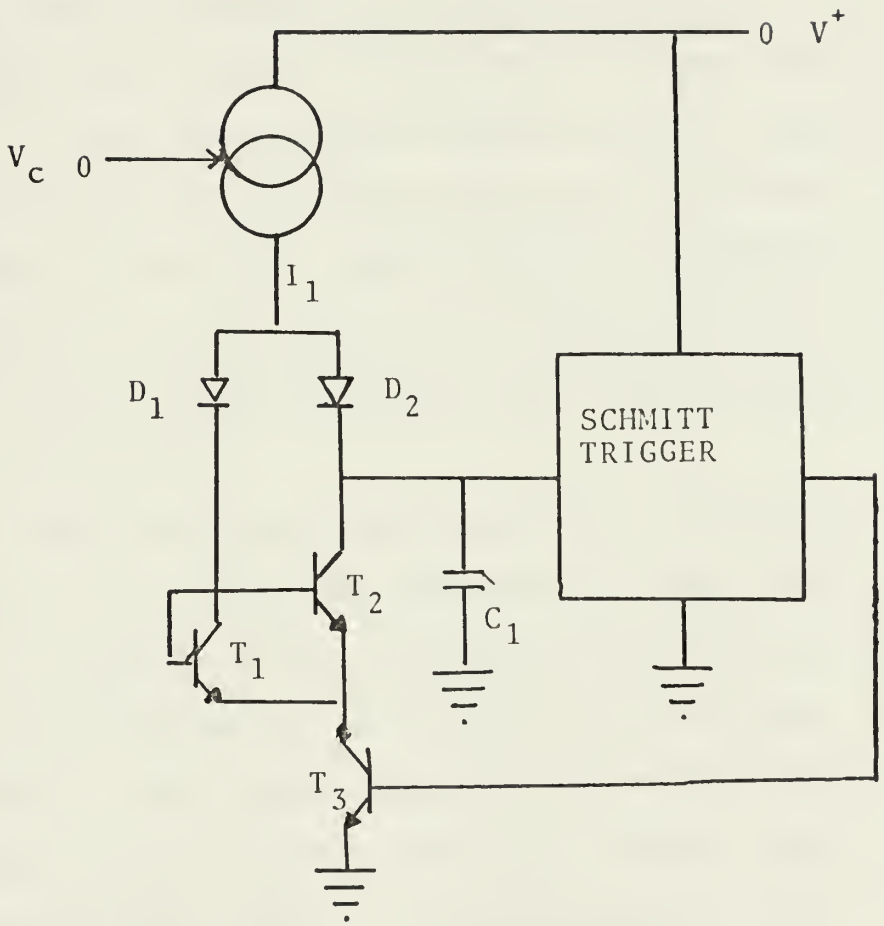

FIGURE 21 VCO BLOCK DIAGRAM.

T_2, causing D_2 to become reverse biased. The charging current I_1 now flows through D_1, T_1 and T_3 to ground. Since the base-emitter voltage of T_2 is the same as that of T_1, an equal current flows through T_2. This discharges the capacitor C_1 until the lower triggering threshold is reached, at which point the cycle repeats itself. Because the capacitor C_1 is charged and discharged with the constant current I_1, the VCO produces a triangle waveform as well as the square wave output of the Schmitt Trigger [Ref. 8].

A 7 kHz notch filter was designed to remove any components of the carrier frequency which may be present in the output signal of the PLL. The circuit was designed with operational amplifier techniques to take advantage of the minimum usage of active components while still retaining good stability and accuracy

The basic operational amplifier configuration for an active filter usually calls for at least one RC arrangement as a feedback network across the operational amplifier and one RC combination in series with each input source. Usually, only two RC networks are needed to produce a second-order transfer function. Higher orders are achieved by cascading several op-amp arrangements [Ref. 9].

For this particular application the following specifications were arrived at: d-c voltage gain of about 15, a reference frequency of 7 kHz at least 30 db down from d-c gain and a second harmonic of the reference frequency (14 kHz) down at least 40 db from the d-c gain. A dual 741 C linear operational amplifier was used with the first notch set at

7 kHz and the second notch set at 14 kHz. However, each network also contains two poles that must be taken into account to meet the high frequency roll-off requirements. It was then decided that the best way to handle this problem was to place a two section RC network on the output of the op-amp and use a parallel RC in the feedback loop to roll-off the high frequency components.

The first stage design is shown below:

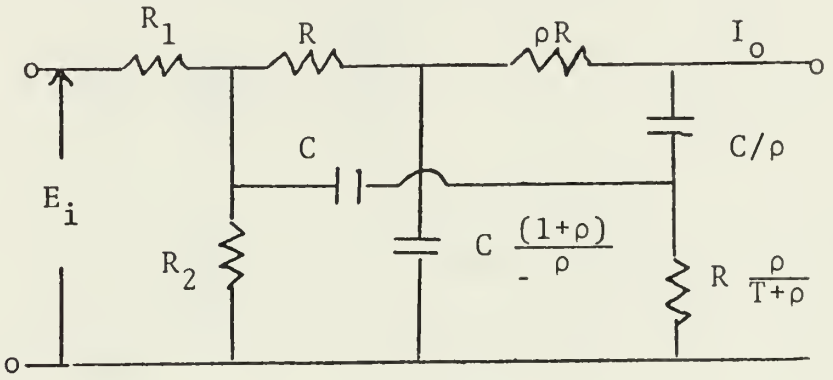

$$T(s) = \frac{K_r(s^2 + \omega_z^2)}{s^2 + \frac{\omega_p}{q_r} s + \omega_p^2}$$

where

$$K_r = \frac{1}{R_1} \qquad \omega_z = \frac{1}{RC}$$

and

$$\omega_p^2 = \frac{[1 + (1 + \rho)a]}{R^2C^2}$$

$$q_r = \frac{1}{1+\rho} \quad \frac{\sqrt{1 + (1 + \rho)a}}{2 + a}$$

$$a = \frac{\frac{R}{R_1R_2}}{R_1+R_2}$$

by substituting for $\omega_z = 2\pi \times 7 \times 10^3$ Hz. We find

$$R = 470 \text{ ohms}$$

$$C = .05 \text{ mfd.}$$

Letting

$$a = 2$$

then

$$R_1 = R_2 = 470 \text{ ohms.}$$

Using

$$\frac{E_o}{E_i} = \frac{y_{21a}}{y_{21b}} = \frac{\frac{\omega_z^2}{R_1 \omega_p^2}}{\frac{1}{R_f}}$$

$$R_f = \frac{15}{y_{21a}} = 63.5 \text{ Kohms and to give a -3db}$$

point about 7 kHz

$$C_f = \frac{2.28 \times 10^{-5}}{6.2 \times 10^4} = 378 \text{ pfd.}$$

The remaining components are all a function of the above derived components and are found below.

$$C_1 = \frac{C(1+\rho)}{\rho} = C\,\frac{4}{3} \quad .0065 \text{ mfd}$$

$$C_2 = \frac{C}{\rho} = \frac{.05}{3} \quad .0167 \text{ mfd}$$

$$R_3 = R\,\frac{\rho}{1+\rho} = 470\left(\frac{3}{4}\right) = 352 \text{ ohms}$$

$$R_4 = \rho R = 1.41 \text{ Kohms.}$$

The completed circuit along with the second state circuit is shown in Figure 22. The second stage circuit used the

same basic design criteria with a unity gain. The completed test results are plotted in Figure 23.

The final stage of the receiver section was the audio amplification of the output from the notch filter. A standard PA-263 audio IC amplifier was used for this purpose. The chip and related circuitry were designed to deliver 3.5 watts of continuous power to a 16 ohm load, although it may be used with a wide variety of load impedances. The IC incorporates two heat sink tabs to dissipate the heat generated on the chip in order to maintain the operating temperatures at an acceptable level.

The amplifier also exhibits low distortion, typically .5 to 2% with a noise level down 70 db. The IC consists of an input circuit of a differential pair of transistors followed by an emitter follower output circuit consisting of a quasi complementary push-pull arrangement composed of NPN and PNP transistors. The circuit utilized is shown in Figure 24. The output of the amplifier is fed into an 8 ohm dynamic speaker for conversion to an audio signal.

The completed receiver is shown in Figure 25(b). The detector window is mounted within the chassis for protection with an opening in the chassis to collect the light signals. Again provisions were made for mounting a telescope on the side to simplify alignment problems when operating the system. The receiver utilizes two 9^{volt} transistor batteries to supply the $\pm 9^{volts}$ required while still maintaining a reasonable battery life.

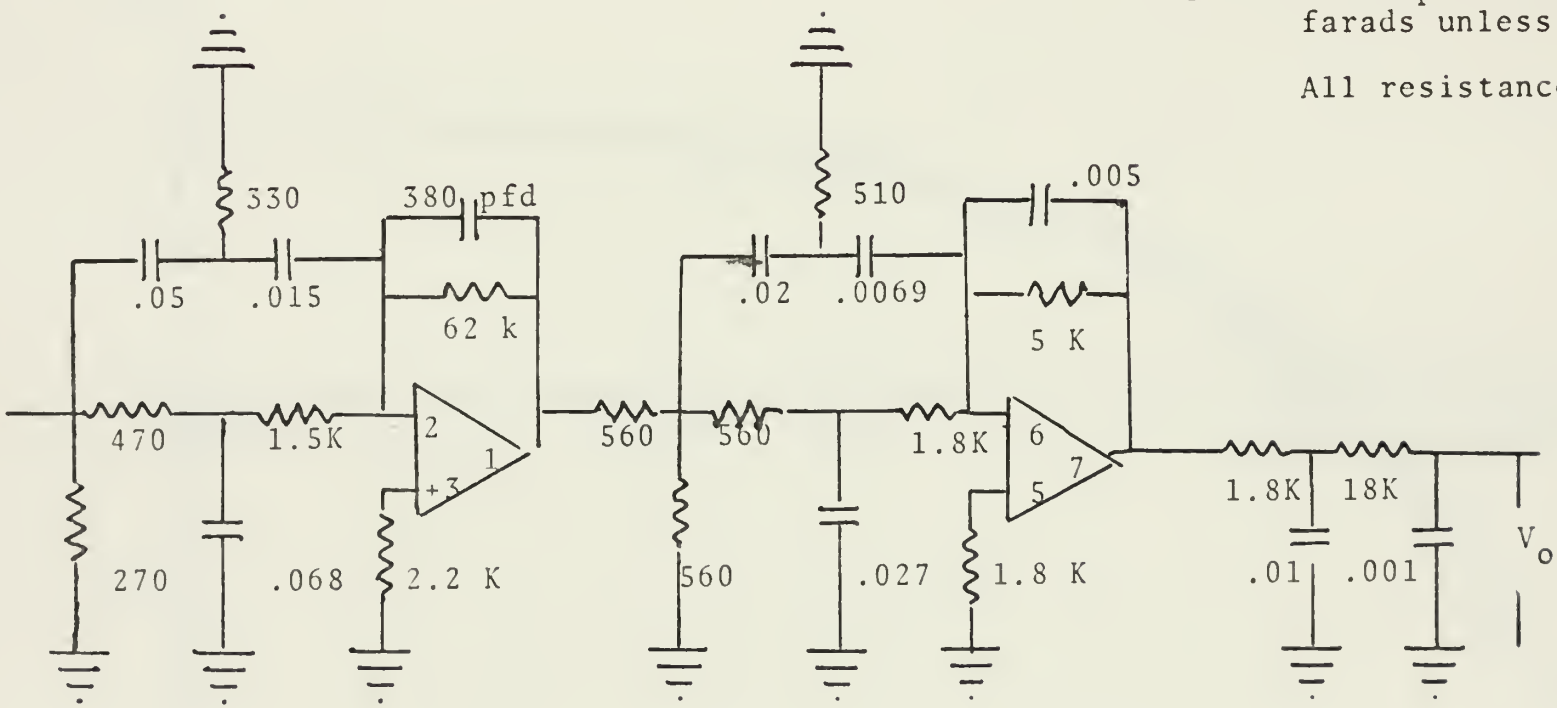

FIGURE 22 NOTCH FILTER CIRCUIT.

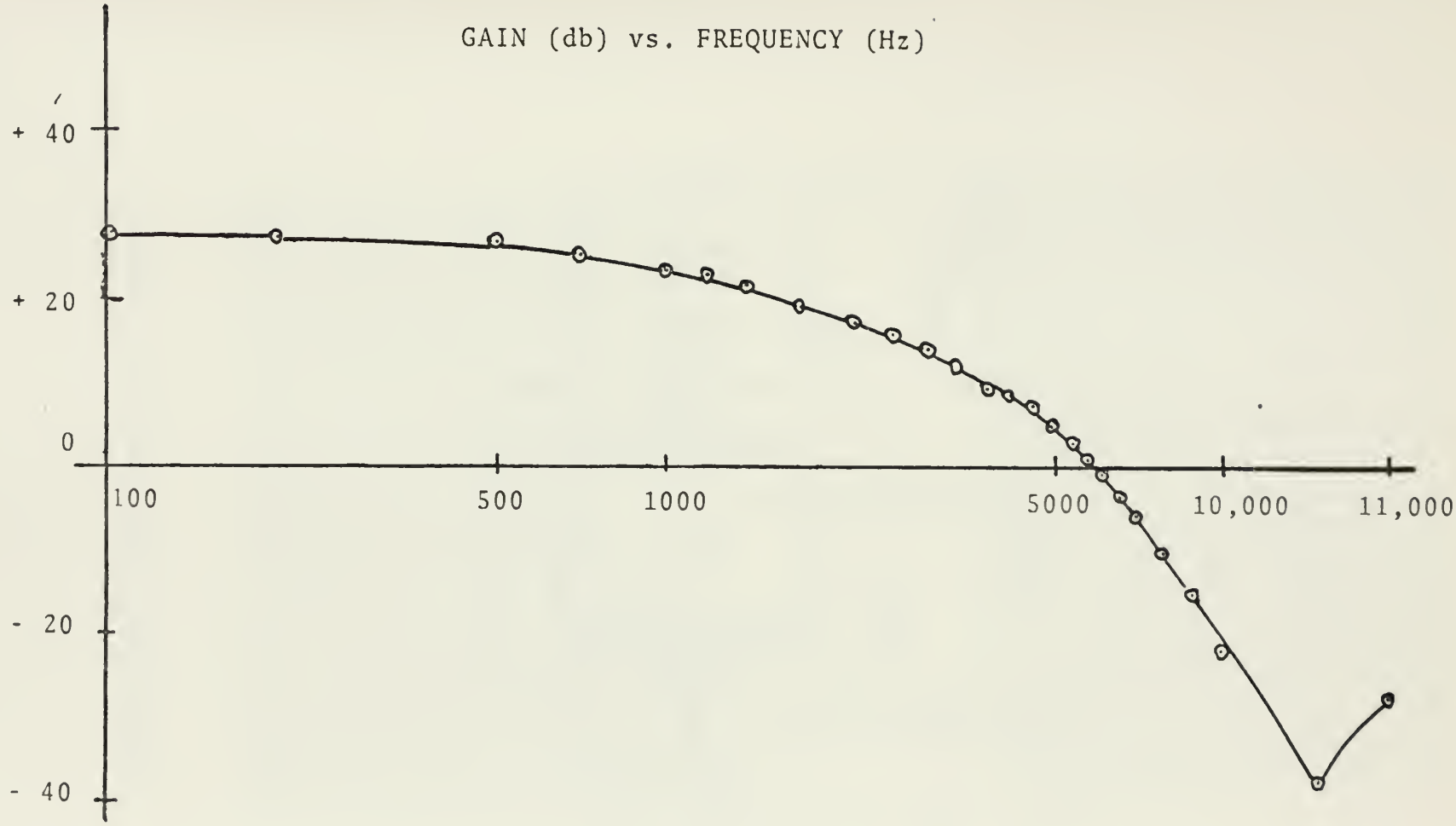

FIGURE 23 NOTCH FILTER FREQUENCY RESPONSE

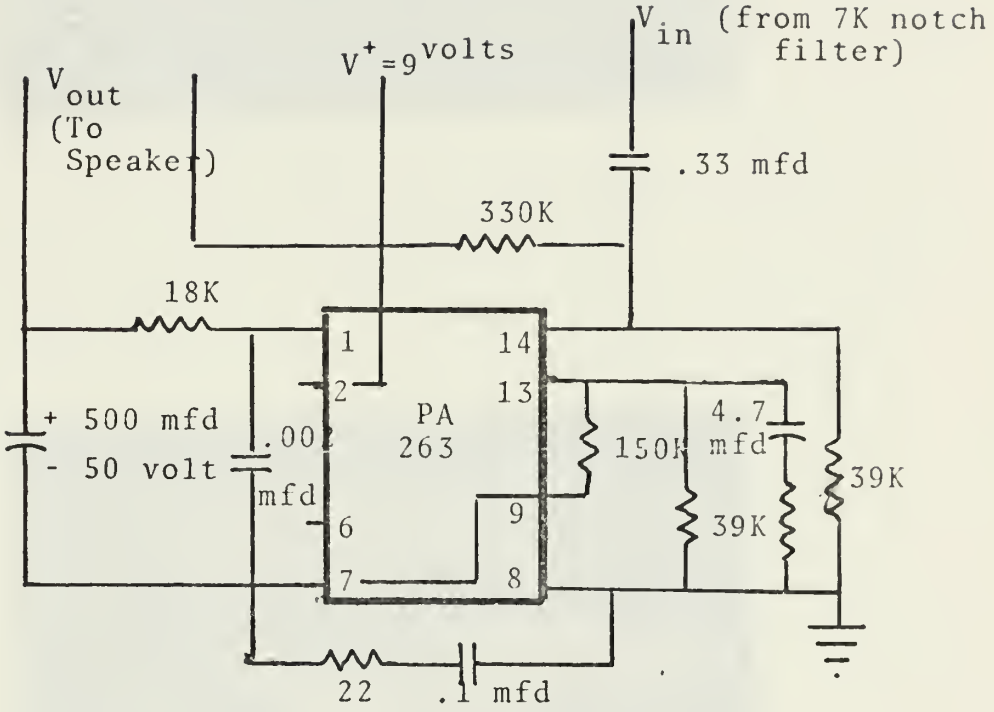

FIGURE 24 AUDIO AMPLIFIER CIRCUIT

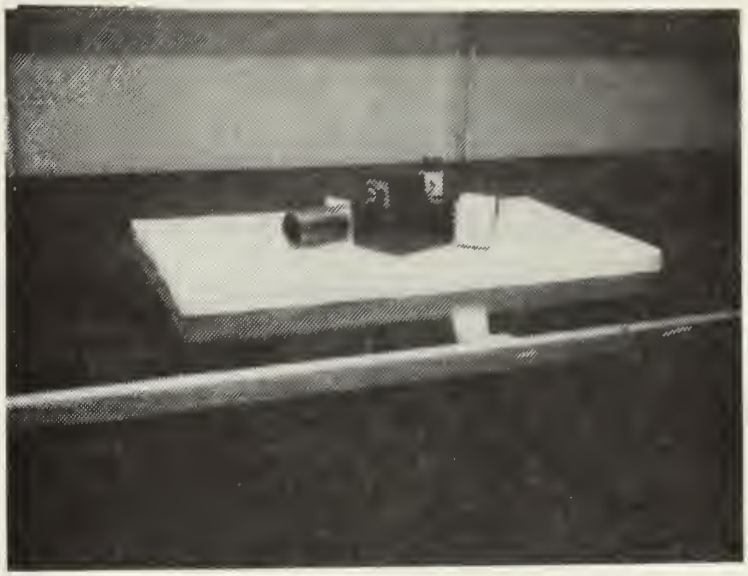

FIGURE [illegible](a) COMPLETED TRANSMITTER

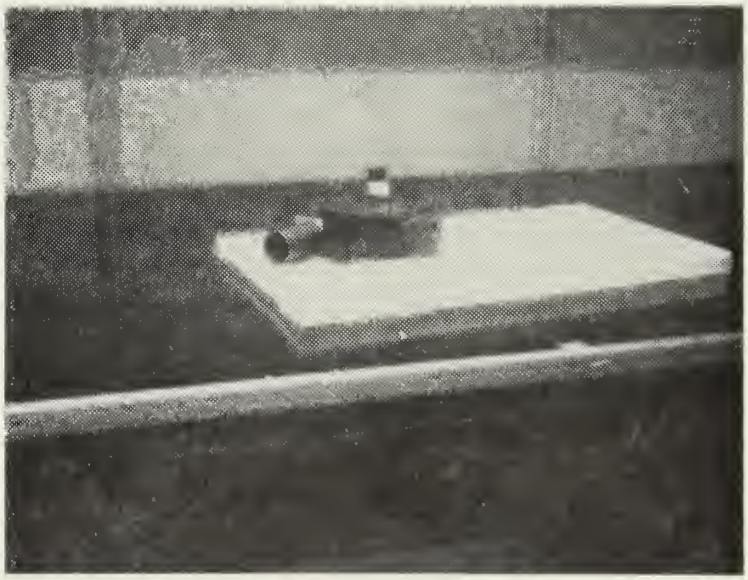

FIGURE [illegible](b) COMPLETED RECEIVER

IV. CONCLUSIONS

The modulation and demodulation schemes were successfully tested with the optical portion of the system bypassed. An audio input from the microphone modulated the VCO and was demodulated via the PLL and it's associated circuitry.

Unfortunately, a failure occurred in the internal circuitry of the TM-6A transmitter during power measurements so the optical portion of the system was not checked out. However the VCO/buffer circuitry/TM-6A system was tested and the system operated as desired with no appreciable waveform distortion.

BIBLIOGRAPHY

1. "The News in Focus," Laser Focus, p. 14, October 1973.

2. Radio Amateur's Handbook, 48th ed., p. 243-245, American Radio Relay League, 1971.

3. Siegman, H. G., An Introduction to Lasers and Masers, p. 48-52, McGraw-Hill, 1971.

4. Medved, D. B., "Photodiodes for Fast Receivers," Laser Focus, p. 45, January 1974.

5. Pankove, J. I., Optical Processes in Semiconductors, p. 302-303, Prentice Hall, 1971.

6. U. S. Department of Commerce/Office of Telecommunications, OT Report 73-3, Optical Communication Systems for Short-Haul Applications, by S. Murahata and L. E. Wood, p. 7, 65, March 1963.

7. Hudson, R. D. Jr., Infrared System Engineering, p. 114-127, Wiley, 1969.

8. Signetics Corporation, A New Phase Locked Loop with High Stability and Accuracy (SE/NE 565) by H. R. Camenzind and J. A. Mattis, p. 7-15, 1970.

9. Welling, B., "Active Filters, Part 6: The Op-Amp Saves Time and Money," Electronics, p. 82-90, 3 February 1969.

10. Halkias, C. C. and Millman, J., Integrated Electronics: Analog and Digital Circuits and Systems, p. 79-85, McGraw-Hill, 1972.

11. Smith, W. V. and Sorokin, P. P., The Laser, p. 368-390, McGraw-Hill, 1966.

INITIAL DISTRIBUTION LIST

		No. Copies
1.	Defense Documentation Center Cameron Station Alexandria, Virginia 22314	2
2.	Library, Code 0212 Naval Postgraduate School Monterey, California 93940	2
3.	Department Chairman, Code 52 Department of Electrical Engineering Naval Postgraduate School Monterey, California 93940	2
4.	Professor C. H. Rothauge, Code 52Rt Department of Electrical Engineering Naval Postgraduate School Monterey, California 93940	1
5.	Asst Professor J. P. Powers, Code 52Po Department of Electrical Engineering Naval Postgraduate School Monterey, California 93940	1
6.	LT John James Sulfaro, USN Attack Squadron Forty-Two NAS Oceana Virginia Beach, Virginia 23454	1

Thesis
S85835
c.1

156857

Sulfaro
A pulse modulated
laser communications
system.